Sensitivity of Field Data and Field Protocols in One-Dimensional Hydraulic Modelling

- A Case Study on Varying Slopes and Channel Roughness -

by

Robert Matthew William Kuta

A thesis
presented to the University of Waterloo
in fulfillment of the
thesis requirement for the degree of
Master of Applied Science
in
Civil Engineering

Waterloo, Ontario, Canada, 2008

AUTHOR'S DECLARATION

I hereby declare that I am the sole author of this thesis. This is a true copy of the thesis, including any required final revisions, as accepted by my examiners.

I understand that my thesis may be made electronically available to the public.

ABSTRACT

Over one million simulations were conducted using the Hec-Ras4b (US Army Corps of Engineers, 2004) model to evaluate the sensitivity of model predictions to field data accuracy, density and estimation techniques and provide guidance towards balancing human resource allocation with model accuracy. Notable differences were identified in model accuracy if a project is concerned with river processes occurring within the limits of the bankfull channel versus floodplain regions. Increased cross section discretization, bankfull channel detail and main channel roughness were of greatest field survey and measurement importance when processes relevant to the bankfull channel are of concern (i.e. geomorphic processes or sediment transport). Conversely, where flood conditions are of highest consideration, estimates of floodplain roughness dominate the accuracy of the results of computed water surface elevations. Results for this case study also demonstrate that higher orders of total station field surveys provide little additional accuracy in final predicted water surface elevations, relative to proper estimates of in-channel and floodplain roughness. As long as drift in field surveys has been accounted for during or subsequent to total station surveys, survey techniques such as hangers can be readily employed with very little increase in final model prediction error, while improving field data acquisition efficiency.

ACKNOWLEDGEMENTS

The Funding for this project was sponsored by the National Scientific and Engineering Research Council of Canada (NSERC) discoveries grant program, the University of Waterloo, Faculty of Engineering, Deans' Graduate Scholarship Awards and by the City of Hamilton.

I would like to thank friends, staff, and faculty at the University of Waterloo for there assistance and support throughout this academic endeavor. A special acknowledgement to my academic advisors Dr. William Annable and Dr. Bryan Tolson for their guidance and sound knowledge in the sciences of open channel hydraulics and numerical modelling – thank you.

For Chris

TABLE OF CONTENTS

LIST OF TABLES

LIST OF FIGURES

LIST OF FIGURES cont…

NOTATION

Symbol	Units	Description
a	[-]	coefficients based on the bending characteristics of vegetation
a_i	[L^2]	calculated panel area used in velocity-area method
A	[L^2]	cross section area
b	[-]	coefficients based on the bending characteristics of vegetation
C	[-]	horizontal discrepancy factor
d	[L]	measured downstream distance
d_s	[L]	bed roughness related particle size
D_x	[L]	particular particle size
D_{50}	[L]	mean particle size
f	[-]	Darcy-Weisbach friction factor
F	[-]	Froude number
g	[L/T^2]	gravitational constant
h	[L]	stem length
h'	[L]	flow depth
h_L	[L]	energy losses between cross sections
H	[L]	total energy
H	[L]	height above a given weir structure
i	[-]	cross-section of interest along the longitudinal reach
k	[L]	height of roughness
K	[L^3/T]	conveyance of the channel
$\overline{K}$	[L^3/T]	average conveyance

NOTATION cont…

Symbol	Units	Description
K_{up}	[L^3/T]	conveyance at upstream cross section
K_{down}	[L^3/T]	conveyance at downstream cross section
K_n	[-]	Strickler coefficient
l	[-]	number of cross sections within a reach
L_S	[L]	stream length along the bankfull channel centre line
L_V	[L]	length of the valley along the valley trend
m	[-]	number of sub-cross-sectional geometric and roughness characteristics of the bankfull channel and associated floodplains
m_5	[-]	factor used in Haestad and Dyhouse's Manning's Estimation approach to correct for the tortuosity of the meander pattern
MEI	[-]	vegetation stiffness
$MWSE_k$	[L]	axiom's water surface elevation at a particular cross section k
n	[-]	manning's roughness coefficient
n_0	[-]	portion of the Manning's n value that represents the channel material
n_1	[-]	portion added to correct Haestad and Dyhouse's Manning's Estimation approach for surface irregularities
n_2	[-]	portion added to correct for variations in the channel shape and size
n_3	[-]	portion added to correct for obstructions in the flow path
n_4	[-]	portion added to correct for vegetation
N	[-]	number of panels for a given top width in the velocity-area Method
p	[L]	wetted perimeter

NOTATION cont...

Symbol	Units	Description
q	[L^2/T]	unit discharge
Q	[L^3/T]	discharge
r	[L]	allowable horizontal discrepancy
R	[L]	hydraulic radius
S_f	[L/L]	friction slope
S_0	[L/L]	channel bed slope
S_V	[L/L]	slope of the valley along the valley trend
t	[T]	time
u_i	[L/T]	channel velocity in the Cartesian coordinate system in principle directions $i = X, Y, Z$
$\overline{U}$	[L/T]	average channel velocity
$\overline{V_i}$	[L/T]	depth-averaged panel velocity used in velocity-area method
WSE_k	[L]	computed water surface elevation at a particular cross section k
x	[L]	elemental length
y	[L]	channel depth
$\bar{y}$	[L]	average flow depth
y_n	[L]	normal flow depth
Z	[L]	elevation datum

Greek

α	[-]	kinetic energy head correction coefficient
ΔE	[L]	change in specific energy
ΔH	[L]	difference in total energy loss

NOTATION cont…

Symbol	Units	Description
γ_W	[M/L^2-T^2]	specific weight of water
θ	[-]	units conversion factor for Manning's equation
τ	[M/T^{2}L]	total boundary shear
Ω	[-]	average sinuosity
ΔX	[L]	cross-section spacing
$\overline{\lvert \in \rvert}$	[L]	average absolute cross sectional water surface elevation error (i.e. main measure of error between experiments)

CHAPTER 1. INTRODUCTION

A trend in the hydraulic modelling community over the past two decades has been a tendency for many practitioners and agencies to dictate high levels of field survey accuracy with the expectation that the accuracy of conventional field survey method protocols will produce the most accurate water surface elevations in hydraulic models. Precise field protocols then relate to project economics, which typically result in a river project limiting the amount of field effort in attempts to reduce project costs while not completely recognizing the tradeoffs in hydraulic modelling accuracy. The sensitivity and resource effort of field methods and protocols need to be better understood in the context of resulting model accuracy and where more simplified methods and protocols may be applied with no sacrifice in simulated water surface elevations.

The initial stages of investment into a hydraulic modelling project from both a time and effort perspective produce desirable gains in the model's computed water surface profile; however, as more time and effort is invested into the project this continued trend in gains does not follow. Reich and Paz (2008) identified an asymptotic relationship between resource investment and project quality whereby the quality of the project does not increase substantially after a certain point with additional human resource or equipment investment. They further identified generic issues for consideration in any hydraulic modelling analysis which included: the level of detail required in the model to ensure success for the intended water course project, available resources (human, funding, equipment etc.), best allocation of resources, and the level of risk of a given project. However, their assessment did not consider the different field techniques, protocols and parameters explicitly when evaluating the cost/economics of a given river project.

The accuracy of the model's outcome is directly related to the quality and quantity of the data used to compute that prediction. In the case of a one-dimensional hydraulic model topography,

roughness, and flow make up the three key input variables that determine how well the model emulates natural flow events.

The topographical data in a one-dimensional model is made up of cross sectional points in space, which are recorded across the channel – perpendicular to the direction of flow. These points are related to each other through the accuracy of their x, y, and z coordinates; therefore, increasing the number of recorded spatial points across a cross section results in a greater representation of the cross section within the model. However, a one-dimensional model assumes a homogeneous topographical transition from one cross section to the next consecutive cross section. This does not take into account the irregularity of the channel itself. What this means is – depending on the irregularity of the channel between cross section – an accurate cross section may not computationally represent the heterogeneity, or irregularity, of the channel between cross sections.

Roughness data, as it relates to this study, is included in the model in the form of Manning's n values. In a one-dimensional model these values are entered for each cross section's left flood plain, main channel, and right flood plain. The values entered into a model are obtained through a combination of field methods and applied theory, as described throughout this report. The likeness of the model's roughness to that of the natural environment is dependent on the number of field samples taken as well as the distance between cross sections.

Finally, the flow data used during the simulation must be entered in a manner that reflects the cumulative nature of the channel's discharge as you travel downstream. The realistic behavior of the model will depend on how many flow change locations are entered – accounting for cumulative flow from runoff and tributaries. The individual flows entered at each flow change location are obtained via the stage discharge curve, which is created from physical measurements of individual flow event as well as stage data acquired over time. The accuracy of the stage

discharge curve, and in turn the accuracy of the model, is related to the number and location of flow measurements taken in the field.

All of this input data is collected via various field methods; therefore, to gain a better understanding of hydraulic modelling input variables this study focuses on evaluating the sensitivity of common input parameters and their corresponding field protocol accuracy to a one-dimensional hydraulic model (Hec-Ras4b, U.S Army Corps of Engineers, 2004). Monte Carlo numerical experiments are conducted on topographic accuracy, cross section resolution and roughness estimation methods and determine the significance of impact on resulting water surface elevations. It is not the intention of this study to examine every input parameter to Hec-Ras, but rather how key parameters and inputs relate to project economics and resource management in the context of resource allocation. To achieve this, the proposed question of this study is as follows:

> Using a physical based hydraulic model, how do input variables – topographic, roughness, and flow – individually affect the model's ability to simulate natural events; and based on these individual effects, how should a modelling project's resources be distributed to ensure optimal hydraulic predictions ensue?

CHAPTER 2. BACKGROUND

The selection and/or development of a model is a choice in how one represents the salient physical, chemical and/or biological processes of an environmental system for a given level of accuracy. Moreover, the accuracy of a given model is largely dependent upon the quantity and quality of data obtained for input, calibration, and validation. Modelling of river systems is akin to such challenges and there are always economic tradeoffs in developing site specific models and the costs related to data acquisition and the intended model accuracy. Dooge (1972) provides a summary of modelling challenges related to hydraulics and hydrology as:

1. a proliferation of approaches and techniques;
2. a further proliferation of models based on any one of these particular approaches;
3. a failure to develop adequate techniques for the evaluation of specific models and for choices between models in a given situation; and
4. a widening gulf between research techniques and operational methods.

Today's practice of modelling a river network usually proceeds down one of two paths being: an empirical approach (also referred to as auto-regressive modelling) or a physically-based approach. The empirical approach involves the collection of large amounts of historical at-a-station hydrometric data at single or multiple observations sites. Data are then analyzed through several statistical methods to develop auto-regressive models (Salas, 1993) and are then forward-cast to predict future flow duration and frequency characteristics for a given watershed and land use. These approaches typically focus on the long-term hydrology trends within a watershed and provide little insight into the changes in hydraulic geometry with varying spatial or temporal boundary conditions. Further, the empirical approaches are applied at watershed scales where available spatial data is often limited to topographic maps or digital elevation models (DEM's) and

under conditions of constant land use (stationary moment assumption) and channel dimensions. Such approaches are then limited when considering the development of a hydraulic model for design purposes, where no historical data exists or channel alterations have occurred with time or are proposed.

Physically-based approaches are derived from the fundamentals of fluid mechanics which incorporate spatial geometric and resistance metrics which can then be used to either model existing or proposed river network conditions. Open channel flow in river channels is often described using the St. Venant Equation for either transient or steady-state flow conditions (Chaudhry, 2008) as defined by:

$$u_i \frac{\partial y}{\partial x} + y \frac{\partial u}{\partial x} + \frac{\partial y}{\partial t} = 0 \tag{2.1}$$

where u_i is the channel velocity (L/T) in the Cartesian coordinate system in principle directions $i = X, Y, Z$, y is the channel depth (L), x is the elemental length (L), and t is time (T). In many cases, however, where the velocity in the longitudinal direction u_X is significantly greater than the transverse lateral (u_Y) or transverse vertical (u_Z) such that $u_x \gg (u_y, u_Z)$ then a longitudinal one-dimensional form of Equation 2.1 can be simplified to:

$$g \frac{\partial y}{\partial x} + u \frac{\partial u}{\partial x} + \frac{\partial u}{\partial t} = g\,(S_O - S_f) \tag{2.2}$$

where g is the gravitational constant (L/T^2), S_O is the channel bed slope (L/L) and S_f is the friction slope (L/L) defined by the energy line slope as defined by:

$$S_f = -\frac{\Delta H}{\Delta X} \tag{2.3}$$

where ΔH is the difference in total energy loss (L) between successive cross-sections of spacing ΔX (L). The total energy H (L) at a given cross-section is defined by:

$$H = Z + \bar{y} + \frac{\bar{U}^2}{2g} \tag{2.4}$$

where Z is the elevation datum (L), $\bar{y}$ is the average flow depth (L), g is the gravitational constant (L/T^2) and $\bar{U}$ is the average channel velocity (L/T) as defined by the Manning's equation:

$$\bar{U} = \frac{\theta}{n} R^{2/3} S^{1/2} \tag{2.5}$$

where R is the hydraulic radius (L) defined by $R = A/P$ where A is the cross section area (L^2) and P is the wetted perimeter (L) for a given discharge Q (L^3/T), θ is a units conversion factor ($\theta = 1$ for S.I. units and $\theta = 1.49$ for imperial units) and n is the Manning's roughness coefficient (-).

For compound channels, Equation 2.5 is comprised of multiple conveyance sections as defined by:

$$Q = \sum_{i,j=1}^{m} Q_{i,j} = \sum_{i,j=1}^{m} \frac{A_{i,j}}{l_{i,j}} R_{i,j}^{2/3} S_{f_{i,j}}^{1/2} \tag{2.6}$$

where m is the number of sub-cross-sectional geometric and roughness characteristics of the bankfull channel and associated floodplains and, i is the cross-section of interest along the longitudinal reach of l cross sections. Included in Equation 2.6 is the expression used to calculate channel conveyance defined by:

$$K_{k,j} = \frac{\theta}{n_{k,j}} A_{k,j} R_{k,j}^{2/3} \tag{2.7}$$

where K is the conveyance of the channel (L^3/T). Combining Equations 2.6 and Equation 2.7 result in a method of calculating the friction slope (S_f) for a given cross section k as:

$$S_{f_k} = \sum_{j=1}^{m} \left(\frac{Q_{k,j}}{K_{k,j}}\right)^2 \quad (2.8)$$

where $\sum_{k,j}^{m} Q_{k,j} \equiv Q$ for all k, where Q is the design discharge of interest (such as a regulatory design discharge, Q_{100}, Q_{50}, Q_{20}, Q_2, etc.) (L^3/T).

Equation 2.6 through Equation 2.8 are solved for a series of cross sections k using the *Standard Step Method* with a series of boundary conditions such as known discharge, critical depth, normal depth while maintaining either conservation of energy or momentum based upon the hydraulics of the channel under sub critical, super critical or mixed flow regime conditions. The resulting solution then provides a unique water surface elevation (WSE) (L) at each cross section *k* which is one of the most common metrics used for model calibration purposes and output parameters for design and regulatory purposes (i.e. flood prone limits).

In obtaining a given WSE, there are a number of input variables that control the accuracy of the computed WSE, namely the hydraulic geometry and roughness elements of each sub-section of each cross section and the Euclidian channel slopes between sections. Further, calibrations metrics such as stage-discharge relationships, critical depth, normal depth, etc., also rely upon a certain level of accuracy from field measurements. Regardless of the input parameters, model output and calibration are directly coupled to the quality and quantity of data obtained which are then a reflection of the human resources and costs associated with data acquisition. The remaining sections of this chapter provide insight into the different methods of data acquisition,

related accuracy, level of effort in acquisition, along with how these data collection methods play out in the overall cost of a water course project.

2.1 Field Inventory Techniques

Spatial data includes both the longitudinal profile of a study reach as well as the channel defining profiles that give a hydraulic model the digital geometry used throughout the one-dimensional calculation of the *standard step* method. The roughness data is made up of both instream and overbank roughness estimations. The methods used to estimate instream and overbank roughness vary due to differences in the two locations' in-situ materials. Discharge data, the key variable for model calibration, is collected via instream structures (i.e. weirs) or through the use of transient methods such as handheld flow meters. The field inventory techniques used to collect all of this model-creation data are detailed in the following sub-sections.

2.1.1 Spatial Data

Spatial data collection methods include air photos, topographic maps (at scales ranging from 1:2,000 to 1:100,000), LIDAR (Light Detection and Ranging), total station surveys, and varying resolutions of GPS technology. With regard to the accuracy of topographical representation, these methods range in resolution and therefore vary in their application to hydraulic modelling.

The lowest resolution resources include topographical maps and air photos. Topographic maps and stereo aerial photo analysis can be combined to provide horizontal resolution on the scale of $\pm 1.5m$ (Haestad and Dyhouse, 2003). A compendium of standards compiled by the U.S. Army Corps of Engineers (USACE, 1994) for the employment of hydraulic models for the purposes of flood zone mapping states that horizontal accuracy shall be such that any definable feature will be $\pm 0.005m$ of its true location when plotted to scale. This translates to a 1:2,000 scale map, derived from an aerial photo, having a horizontal accuracy of $\pm 1.0m$. The same standards state that contours shall be ¼ of the contour interval, such that a 1 m contour line interval would be

expected to have a vertical accuracy of $\pm 0.5m$ and a 1.0 m spot elevation would be expected to have a vertical accuracy of $\pm 0.25m$ (Fowler, 2002). The resulting resolution provides a good characterization for valley and floodplain characteristics; however, as many agencies require WSE's in association with flood prone mapping to be vertically within $\pm 0.1m$, limitations exist in exclusively using this resource based information. Conversely, due to readily accessible and low cost of the information, it does offer the ability to conduct a large scale hydraulic analysis where estimations of macro hydraulic effects are sufficient.

LIDAR can also be used to obtain spatial data for hydraulic modelling. LIDAR uses optical remote sensing technology to map the topography of the ground surface via a flight pass. The resolution at which LIDAR data is collected is to maintain a standard of $\pm 0.1m$ (Natural Resources Canada 2005). A common problem, however, in using LIDAR to collect spatial data is that it cannot penetrate through vegetation or under water. This can create significant problems in estimating ground elevations and is then directly coupled to the variability in floodplain vegetation height (which can range between 0m – 30m). These issues can be partially overcome in many environments where LIDAR surveys are taken in the winter when deciduous vegetation is dormant and there is less reflection off of vegetative cover. Further, with no ability for LIDAR to penetrate through water, characterization of the bankfull channel still requires field survey techniques that cannot be conducted remotely.

Two contemporary methods of acquiring spatial field data for both the floodplain and bankfull channel limits, and of the highest accuracy, include total stations surveys (which is comprised of a theodolite, infra red measuring device and reflecting prisms) and global positioning systems (GPS). Contemporary total stations are commonly horizontally and vertically accurate to within $\pm 0.003m/100m$ and $\pm 0.005m/100m$ respectively whereas the most accurate differential GPS

systems commonly have horizontal and vertical accuracies to within $\pm 0.010m$ and $\pm 0.020m$ respectively under ideal operating conditions of a discrete spatial location. A challenge does exist in the employment of GPS technology within river corridors as the systems do not work effectively under dense tree canopy (which is common in river corridors). Therefore, GPS cannot be reliably undertaken at all sites, whereas total station surveys can be conducted in all conditions.

A detailed longitudinal survey of a river channel, which is required in characterizing the variability in channel bed slope, can be obtained by a *traverse topographical survey* (Kavanagh and Bird, 1989) using either of the above noted technologies. The traverse survey constitutes the main longitudinal spatial accuracy of a river survey and is comprised of distance and angle measurements between numerous control-points (commonly referred to as benchmarks or turning points) located along the study reach of interest. In practice, a traverse survey can be one of two types – an *Open Traverse* or a *Closed Traverse*, as illustrated in Figure 2-1.

An open traverse is defined as a series of measurements obtained along a specific path which never geometrically closes upon the starting location.[1] This method is commonly used in river surveys as a river never closes back on itself. Conversely, a closed traverse is a survey that geometrically closes back on itself to create a polygon loop. A closed traverse, therefore, can more readily identify survey error within the traverse of the polygon as the beginning and ending locations should be the identical spatial coordinate. Any difference in the spatial data for these two points will be the result of error accumulated during the entire survey.

[1] An open traverse is sometimes referred to as a *Route Survey* and is used in river engineering to capture sections of a river known as *hangers* where no control points are available to close on.

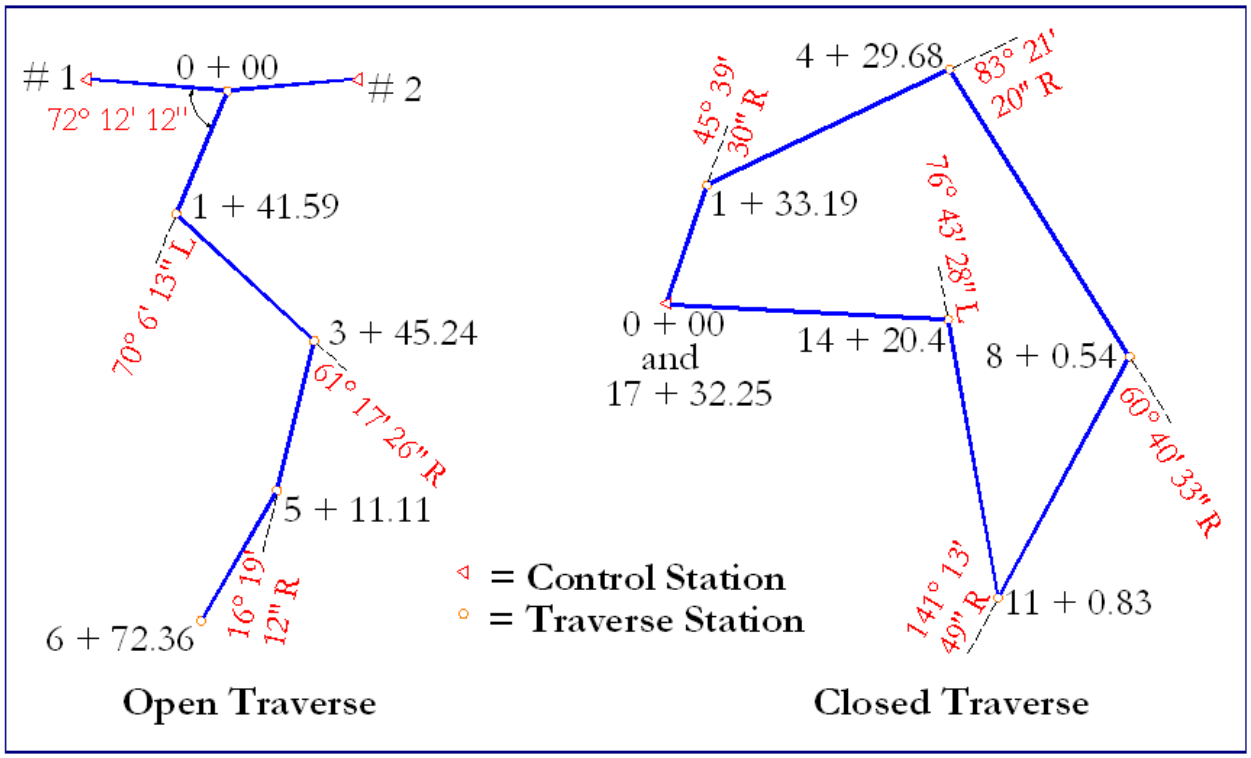

Figure 2-1. Open & Closed Traverse.

Surveying standards identify different levels of surveying accuracy depending upon the data needs, which are identified as special-order, first-order, second-order, third-order, or a forth-order level surveys. The vertical standards for the various orders of surveying are illustrated in Table 2-1 (Natural Resources Canada, 1978). The acceptable horizontal discrepancy is determined using Equation 2.9 where r is the allowable horizontal discrepancy (L), C is the horizontal discrepancy factor (listed in Table 2-2 for the various survey orders), and d is the measured downstream distance (L). In Canada, these tolerances are used in control surveys where results must be within second order horizontal tolerance and a third order vertical tolerance (Canada Centre for Cadastral Management, 1997).

Table 2-1. Vertical Allowable Discrepancies for Various Orders of Surveys.

Survey Order	Allowable Vertical Discrepancy
Special	$\pm 3 \text{ mm} \times \sqrt{K}$
1st	$\pm 4 \text{ mm} \times \sqrt{K}$
2nd	$\pm 8 \text{ mm} \times \sqrt{K}$
3rd	$\pm 24 \text{ mm} \times \sqrt{K}$
4th	$\pm 120 \text{ mm} \times \sqrt{K}$

* where K is the measured downstream distance (km).

$$r = C(d + 0.2) \tag{2.9}$$

Table 2-2. Horizontal Discrepancy Factors.

Survey Order	C
1st	2
2nd	5
3rd	12
4th	30

The open traverse method which is commonly employed in river surveys often requires more stringent field methods compared to the closed-traverse method to ensure the accuracy of the recorded data. These field methods translate to higher orders of surveying which include a practice known as *Double-Faced Surveying* at each of the control points where the distance between points is measured twice (i.e. once in each direction in combination with an instrument optical inversion). Alternatively, or in addition to total station surveys, first-order differential GPS's can also be used at each of the control points to reconcile traverse survey errors arising from the total station methodology. Such additional effort and resources then become more taxing with respect to human resource time in the field because many more steps and often more equipment are required.

The topographical component of the traverse survey is then undertaken from each of the control points of the traverse survey to characterize the reaches spatial characteristics of both natural and manmade elements. Such features include floodplains, terraces, valley limits, tops and bottoms of the bankfull channel, channel geometry, thalweg, levees, tributaries, bridges, culverts, instream structures, in addition to any other features that may affect the hydraulic outcome of the model.

With all the spatial data collection methods identified in this segment, error can manifest itself in the recorded data through a number of ways. In regard to total station surveying, small measurement errors can result from an uncalibrated instrument or a prism pole not being level when a signal is returned; however, the more significant errors and those of most concern usually results from equipment setup and user error. For example, if a prism pole is set to an incorrect height (which commonly occurs) or an incorrect instrument or prism pole height is recorded in the data logger (which commonly occurs) significant error and/or drift in cumulative error can occur. This level of error can affect the performance of the hydraulic model as illustrated later in this report.

2.1.2 Cross-Section Detailing

As previously described, cross sections – another form of spatial data – are fundamental features in defining a hydraulic model. Discrete spatial data at each cross section can be obtained in the topographic total station survey as described in Sub-Section 2.1.1. Alternatively, where repetitive surveys are required within the limits of the bankfull channel to evaluate rates of channel erosion in both transverse vertical and transverse lateral directions (relative to the flow direction) over time, a more time efficient *Level and Graduated Stadia Rod* method is often employed (as illustrated in Figure 2-2).

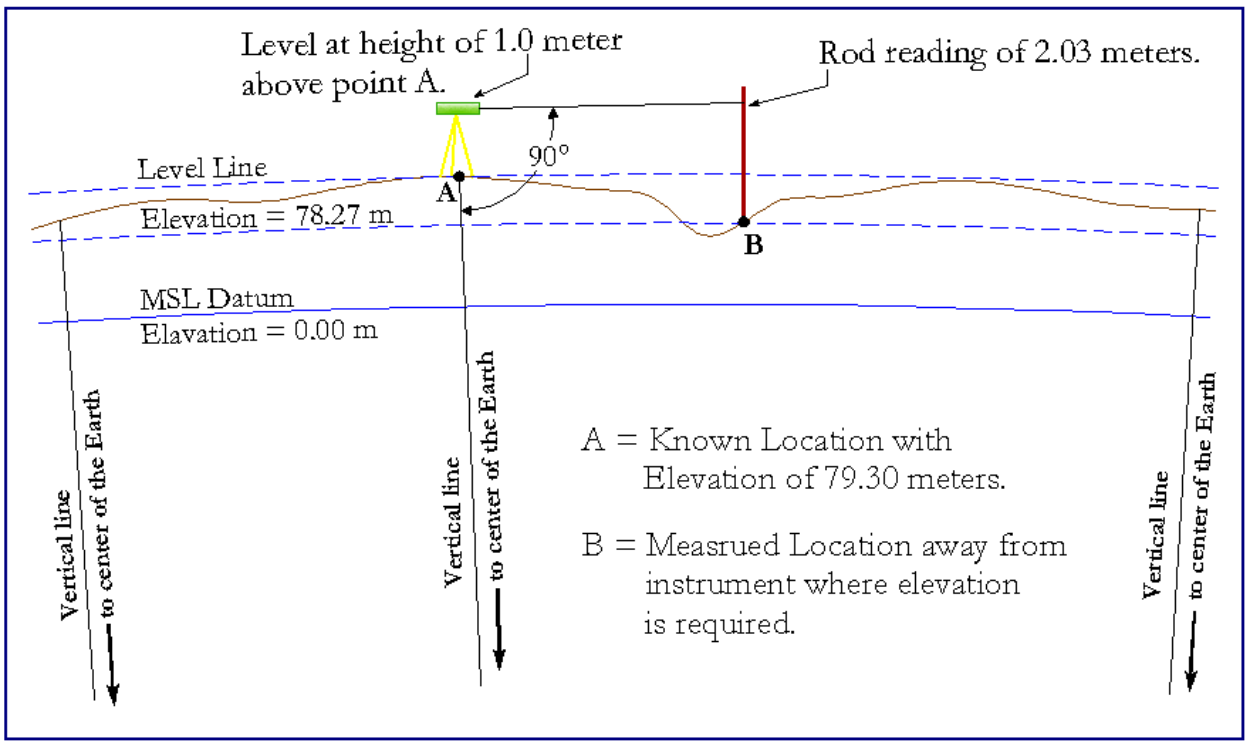

Figure 2-2. Working Example of Leveling.

The level and graduate stadia rod method relies upon bench marks established on either side of the bankfull channel that have been spatially determined using the total station or GPS surveys. A steel tape measure is spanned between the two bench marks and vertical measurements taken (as illustrated in Figure 2-3), using the level (manual or digital) and stadia rod, at consistent horizontal spatial intervals (which range depending upon the width of the channel between 0.5m and 50m) in addition to every notable change in channel bed slope. The vertical elevation at each discrete survey point is then related to the benchmarks established at each cross-section less the observed backsight reading at the height of the level instrument. Standard survey levels are vertically accurate to $\pm\ 0.002m/100m$ with stadia rod gradations of $0.0025\ m$.

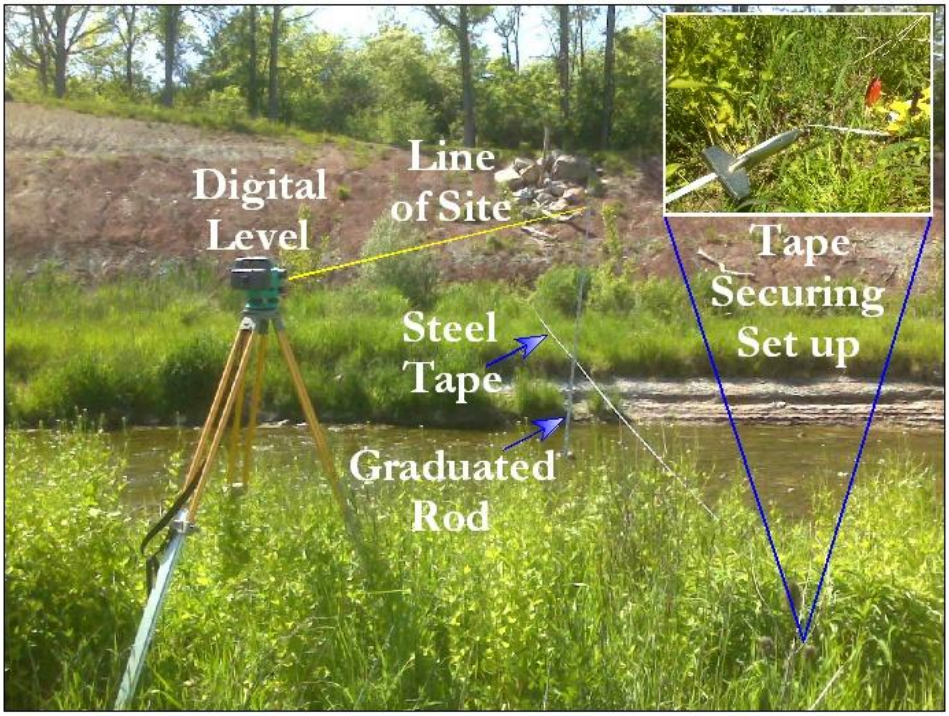

Figure 2-3. Typical Field Setup for Leveling.

In the case of a manual level, the operator looks through the optics of the instrument and reads the height of the graduated rod at the point where the cross-hairs of the optics intersect the rod. This practice involves manually recording and calculating elevation differences post leveling. The digital level offers a much more efficient method of measurement and data collection. With a digital level, the level is centred on a bar coded stadia rod. An image is then taken and the bar code is processed, which is translated into a vertical elevation above the observation point. This allows the operator to observe the elevations without taking time to perform any calculations. This technique eliminates operator miss-read error, and the data is electronically stored in a data logger such that data transcription errors are also eliminated.

Similar to the errors associated with total station traverses as mentioned in the previous section, most leveling errors arise from improper equipment setup. For example, if the height measurement of the level above the known location is incorrect, the elevation of the instrument

will be incorrect and subsequently all of the elevations for the measured locations will be incorrect. Another common error in the leveling process is the poor attention to slope changes within a given cross section (Figure 2-4). When a notable slope change is omitted in characterizing cross sectional geometry, subsequent analysis may result in poor agreement between observed and modelled flows and elevations (WSE's) for specific discharge return periods, in particular for flow conditions ranging between low flow and bankfull discharge.

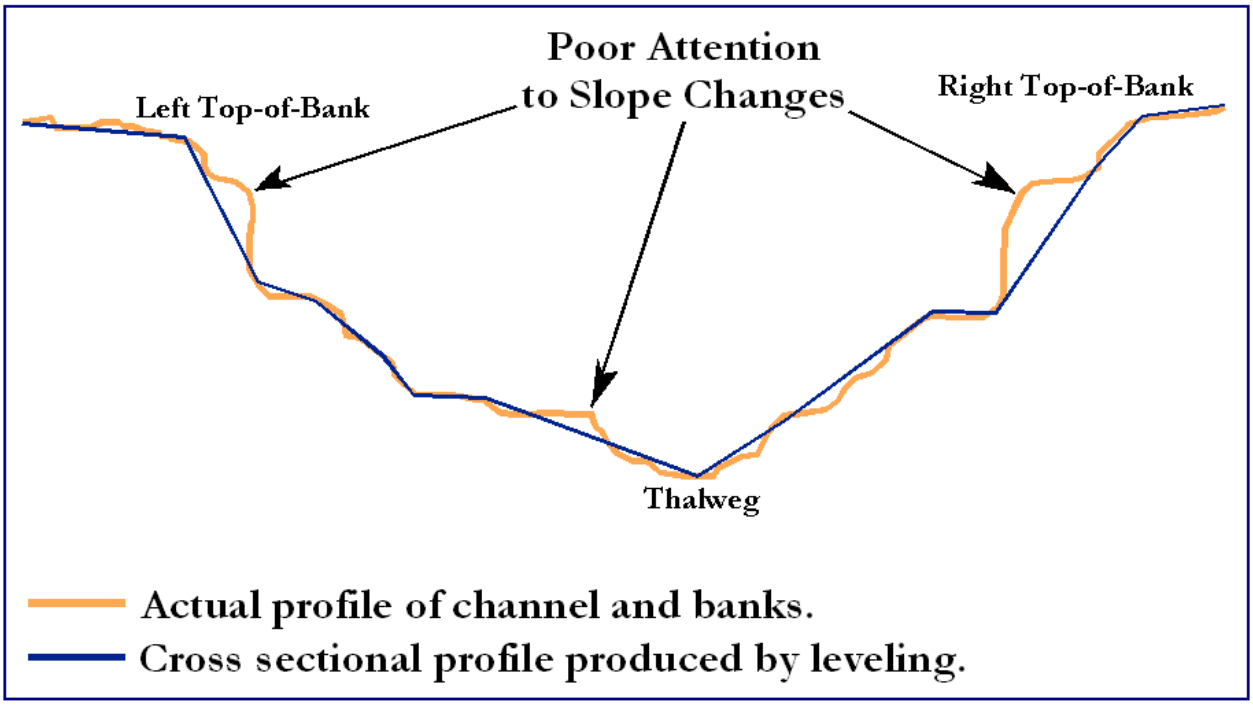

Figure 2-4. Example of Poor Attention to Cross Section Slope Change.

2.1.3 Section Roughness

Similar to the myriad of surveying techniques to quantify the topographic conditions, several techniques are available to estimate channel and floodplain roughness. Such methods include visual estimates (by experienced practitioners), visual comparisons to published literature (such as Chow, 1959, Mason and Hicks, 1991, Annable, 1996), and by field measurement techniques and analysis, such as those offered by Kowen, 1992, Julien, 2002, and Haestad and Dyhouse, 2003.

Literature such as Chow (1959) provides detailed descriptions of various surfaces and what their respective ranges are in Manning's n values. This information can be visually compared to a particular study site and roughness values assigned. Visual estimates, however, are very subjective and considering the range in Manning's n roughness coefficients between concrete n=0.012 and large woody debris on flood plains $0.1 \leq n \leq 0.9$ (Chow, 1959), a two-order range in estimated roughness can have a significant impact upon simulated WSE's.

A complicating issue with roughness values, both instream and overbank, is that the values vary with flow depth, however, model parameterization typically only allows for a single roughness value regardless of depth within a sub-section of a channel. For example, if flow has entered into the floodplain and is passing through a vegetated floodplain, the roughness will be different when flowing between the caliper stalks of vegetation as opposed to larger flow depths passing through the predominate foliage. Kouwen (1992) proposed a method to address such variability for grasses by approaching roughness from a vegetative stiffness and effective roughness height perspective. In this method roughness is characterized by the Darcy-Weisbach relationship as:

$$f = \left(\frac{1}{a + b \log_{10}\left(\frac{y_n}{k}\right)} \right)^2 \tag{2.10}$$

where f is the Darcy-Weisbach friction factor (-), a (-) and b (-) are coefficients based on the bending characteristics of the vegetation which are both functions of the ratio of shear velocity to critical shear velocity [See Kouwen (1992) for list of values], y_n is the normal flow depth (L), and k is the height of roughness (L) as defined by:

$$k = 0.14h \left[\frac{\left(\frac{MEI}{\tau}\right)^{0.25}}{h} \right]^{1.59} \tag{2.11}$$

where h is the stem length (L), MEI is the vegetation stiffness related to the stem length (-), and τ is the total boundary shear (M/T^2L) as defined by:

$$\tau = \gamma_W y_n S_0 \tag{2.12}$$

where γ_W is the specific weight of water (M/L^2-T^2). The Darcy-Weisbach values obtained can then be converted to Manning's n roughness values using the identity:

$$\sqrt{\frac{8g}{f}} = \frac{R^{1/6}}{n} \text{ (S. I. Units)} \tag{2.13}$$

where R is the hyraulic radius as previously defined.

The vegetation stiffness (MEI) can be defined for either green grass or dormant grass as:

$$MEI = 319h^{3.3} \tag{2.14}$$

$$MEI = 24.5h^{2.26} \tag{2.15}$$

respectively. This approach allows hydraulic modellers the ability to obtain roughness estimations via a thorough field reconnaissance where local assessments can be made for the required input variables. This estimation method is most applicable to overbank flows but also offers some utility within the limits of the bankfull channel where dense vegetation may persist (i.e. bulrushes, reeds, etc.).

Another factor that may alter the accuracy of the calculated floodplain roughness coefficient is the species homogeneity and density assumptions used in the estimation approach. For example, it is not feasible to sample every plant species within the floodplain and therefore the homogenous stiffness and height assumptions will only be representative of a single species samples (assumed

to be the highest density species). This single characteristic may represent the mean situation but will not account for variability is species taxa and density with varying roughness (i.e. a downed tree or other debris) at a given cross section. This can be partially overcome by further sub-dividing the flood plain into additional sub cross sections represented in Equation 2.6 if significant heterogeneous floodplain roughness is deemed important in the hydraulic analysis.

Within the limits of the bankfull channel where the wetted perimeter of the channel is principally comprised of bed material and the surrounding geology, Julien (2002) offers a depth varying roughness relationship also based upon the Darcy-Weisbach friction factor of the form:

$$\sqrt{\frac{8g}{f}} = 5.75\ log\frac{2h'}{d_s} \tag{2.16}$$

where h' is the flow depth (L) and d_s is the bed roughness related to particle size (L). For the majority of rivers in southern Ontario (where the current study has been conducted) the relationships between flow depth and bed roughness demonstrate a linear trend in the range of $100 < h'/d_s < 10{,}000$ (Annable, 1996). This linear trend can be adequately represented using Equation 2.5 and the Manning's n value calculated using the simplified Strickler (1923) equation of the form:

$$n = 0.064 D_{50}^{1/6} \tag{2.17}$$

where D_{50} is the mean particle size (in meters) based upon a grain size analysis within the limits of the bankfull channel.

Wolman (1954) offered a pebble count procedure for characterizing the particle size distribution of the bed material within the limits of the bankfull channel which is commonly employed to

populate Equation 2.17 at each cross section. This approach randomly samples the bed material along the wetted perimeter of the channel measuring the B-Axis (Figure 2-5) of each particle sampled. The B-axis is considered the average size class that would pass through a given particle size sieve (Friedman and Sanders, 1978) to produce a cumulative sediment distribution graph.

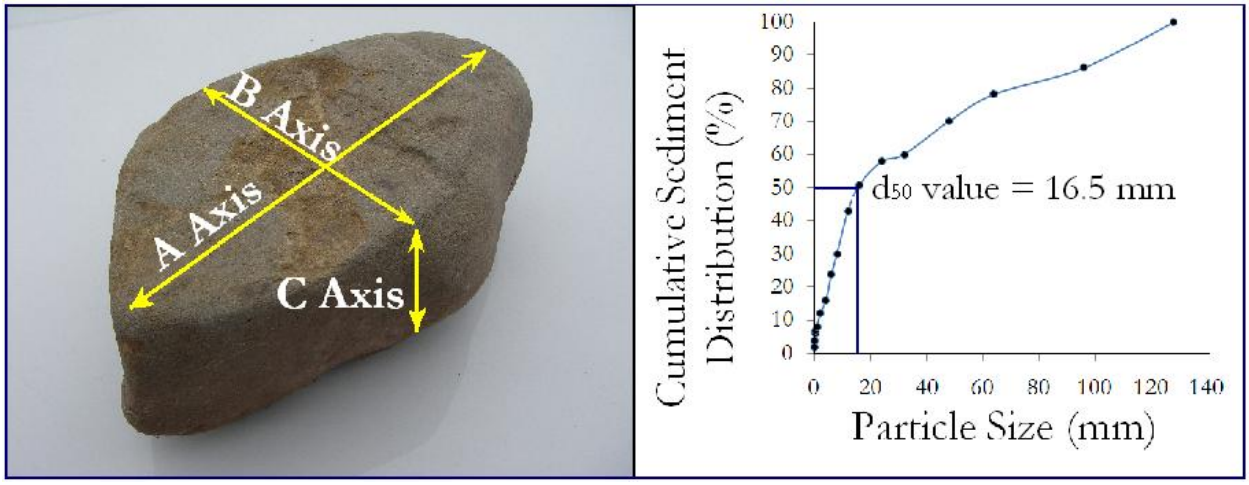

Figure 2-5. Typical Stream Grain Sample & Cumulative Grain Size Distribution.

Once the pebble count data for a cross section has been collected and analyzed, various forms of the Strickler (1923) Equation (Equation 2.18) can be used to calculate Manning's n roughness values of the general form (Anderson et al., 1968):

$$n = K_u \, D_x^{1/6} \tag{2.18}$$

In this equation K_u is the Strickler coefficient and D_x is a particular particle size dependent on the research approach employed. Various research approaches have been carried out and have proposed different values for *Ku* such as those of: Chow (1959), Anderson et al. (1970), Lane & Carlson (1955), and the United States Army Corps of Engineers (1991). Depending on which of these aforementioned approaches are used, slight variations in the calculated baseline manning's n value will result. Chow (1959) values tend to be the lowest roughness estimations whereas United

States Army Corps of Engineers values (Mooney, Holmquist-Johnson, and Broderick 2007) tend to be the highest due not only to the K_u values used but also the fact that a D_{50} grain size is used for Chow's approach whereas a D_{90} grain size is used for the U.S.A.C.E's approach.

Another approach to estimating a Manning's roughness within the limits of the bankfull channel was offered by Haestad and Dyhouse (2003) which combined lookup-table roughness values (Chow, 1959) in conjunction with the Cowan (1956) Equation as defined by:

$$n = (n_0 + n_1 + n_2 + n_3 + n_4)m_5 \tag{2.19}$$

where n_0 is the portion of the Manning's n value that represents the channel material, n_1 is a portion added to correct for surface irregularities, n_2 is a portion added to correct for variations in the channel shape and size through the reach, n_3 accounts for obstructions in the flow path, n_4 accounts for vegetation, and m_5 is a factor that is used to correct for the tortuosity of the meander pattern.

Contrary to traverse and topographic survey errors, roughness coefficients are estimations based on visual observations and interpretations and sampling rather than recording of a series of discrete points. Therefore, factors that may contribute to the bias of these estimations include non-representative grain size sampling during the pebble count procedure at one or a series of cross sections leading to skewed grain size distributions. Skewed grain size distributions often result from observers oversampling larger grain sizes in the field (Rice and Church, 1996) and especially in underwater conditions where the smaller particles are harder to sample and more easily overlooked. A non-representative grain size sample will alter the D_x values obtained in a grain size analysis which will result in a bias in the calculated Manning's n value.

All of these roughness data collection methods require various levels of field efforts which range from simple observation to detailed sampling and measuring. The observational work can be performed through studying photographs or site visits to obtain a qualitative understanding of the vegetation and materials that comprise the channel and floodplain. The more detailed sampling and measuring efforts, on the other hand, require substantially more human resource time but provide a more consistent roughness characterization method.

2.1.4 Discharge Measurement

An important calibration parameter in a hydraulic models development is relating stage data to discharge over a range in flow events. Stage data are obtained at locations of hydraulic control (typically by use of a pressure transducer) which are then related to a series of field measured discharge events producing a stage-discharge curve. Stage obtained from pressure transducers ($\pm\ 0.003m$) is then related to discharge measurements, which can be obtained via numerous methods such as the velocity-area method, slope-area method or control weirs. Each method of discharge measurement offer varying degrees of accuracy and are also dependent upon the human resources and costs associated with each methodology.

One of the most common methods of determining the channel discharge is by the velocity-area method (Buchanan and Somers, 1969). This approach divides the flowing top width of a channel into a series of sub sections, transverse lateral to the mean average flow direction, known as panels. At each panel divide, channel velocities and flow depths are measured and the panel discharge determined. The total discharge of the channel is then determined by:

$$Q = \sum_{i=1}^{N} Q_i = a_i \overline{V_i} \tag{2.20}$$

where N is the number of panels for a given top width (-), a_i is the calculated panel area (L^2), and $\overline{V_i}$ is the depth-averaged panel velocity (L/T). This method is quite easy to perform accurately in a

prismatic channel; however, when larger irregularity occurs (such as a natural channel) errors in discharge measurement increase. Buchanan and Somers (1969) state that with calibrated velocity meters, the average minimum discharge error that can be consistently obtained is $\pm 2\%$ of the actual discharge (which are the standards maintained by the U.S. Geological Survey and Environment Canada). However, if the standards and methods offered by Buchanan and Somers (1969) are not rigorously followed (which commonly occur in the consulting community which is related to human resources and costs) discharge measurement often vary by $\pm 2\% - \pm 20\%$ of the actual discharge. Regardless of the level of effort, this method is also considered to be one of the most taxing with respect to human resource time.

Several flow meters exist to acquire velocity measurements which are commonly used in the velocity-area method which include: horizontal axis meters, vertical axis meters, and acoustic doppler profilers (ADP's), among others. The horizontal axis meter consists of a small propeller attached to a horizontal drive shaft, which is placed in the channel such that the propeller is facing directly into the flow. Revolutions of the propeller are then related to a given calibrated velocity. Common types of horizontal axis meters include the *Swather* and *OTT* meters and are considered accurate to within $\pm 2\%$ of the actually velocity if pointed directly into the flow field. If deviations from the user selected orientation of the flow field occur (a common user error) observed velocities can easily vary between $\pm 10\%$ of the actual point velocity. Alternatively, the vertical axis meter consists of a rotating wheel spinning about a vertical axis with a directional fin on the lee end of the meter. This allows an accurate point velocity to be recorded regardless of the orientation – thus minimizing user error. Some common types of vertical axis meters include the *Price* and *Gurley* meters which are considered accurate to within $\pm 1\%$ of the actual point velocity if properly calibrated and maintained.

Figure 2-6. Example of 2D Acoustic Doppler Profiler.

An alternative to the mechanical flow meters mentioned above are a suite of ADP's. These technologies are based upon pulses emitted from a transmitter located on the flow meter at a range of frequencies (pings) which reflect off of the particulate matter within the water column to three receivers providing a three-dimensional point velocity vector (as illustrated in Figure 2.6), whereas the previously described mechanical velocity meters provide a one-dimensional averaged velocity. The tacit assumption in the application of the ADP's is that the suspended particulate matter within the water column is traveling at the same velocity as the water, and in most cases is a reasonable assumption. ADP technology is typically capable of measuring velocities to within $\pm 0.03\%$ of the actual observed point velocity.

The slope area method is another widely utilized approach for estimating channel discharge (particularly under flood flow conditions). This method employs the Manning's Equation

(Equation 2.5), the conveyance equation (Equation 2.7) and the Strickler Equation (Equation 2-6). High water marks are indicated at two successive cross sections in the field separated by a distance ΔX using the criteria outlined Dalrymple and Benson (1967). Subsequent to the discharge of interest receding, the two cross sections are surveyed in the field to define their geometry and a pebble count conducted is conducted to characterize the Manning's n roughness (Equation 2-6). An average conveyance $\overline{K}$ is calculated between the successive cross sections k_{up} and k_{down} defined by:

$$\overline{K} = \sqrt{K_{up} K_{down}} \tag{2.21}$$

for mild slope channels (i.e. Fr<1) where K_{up} and K_{down} are the conveyance values for the upstream and downstream cross sections (L^3/T), respectively. The water surface slope (S_W) between cross-sections is then used to initially estimate the friction slope S_f and Equation 2.8 is employed to calculate the discharge Q. An iterative approach is then applied to Equations 2.6 through Equation 2.8 to update the discharge to reflect the velocity head of the channel and the final friction slope S_f. If care is taken in parameter estimation and reach selection, this method is considered accurate to within $\pm 10\% - \pm 20\%$ of the actual discharge.

Permanent structures such as weirs and culverts can be installed on streams and rivers to measure discharge. Weirs include sharp-crested weirs, broad-crested weirs, and v-notch weirs as illustrated in Figure 2-7. The unit discharge (q) (L^2/T) of the suite of weirs can then be related to the upstream flow depths H_S, H_b or H_n, as illustrated in Figure 2-7 as follows:

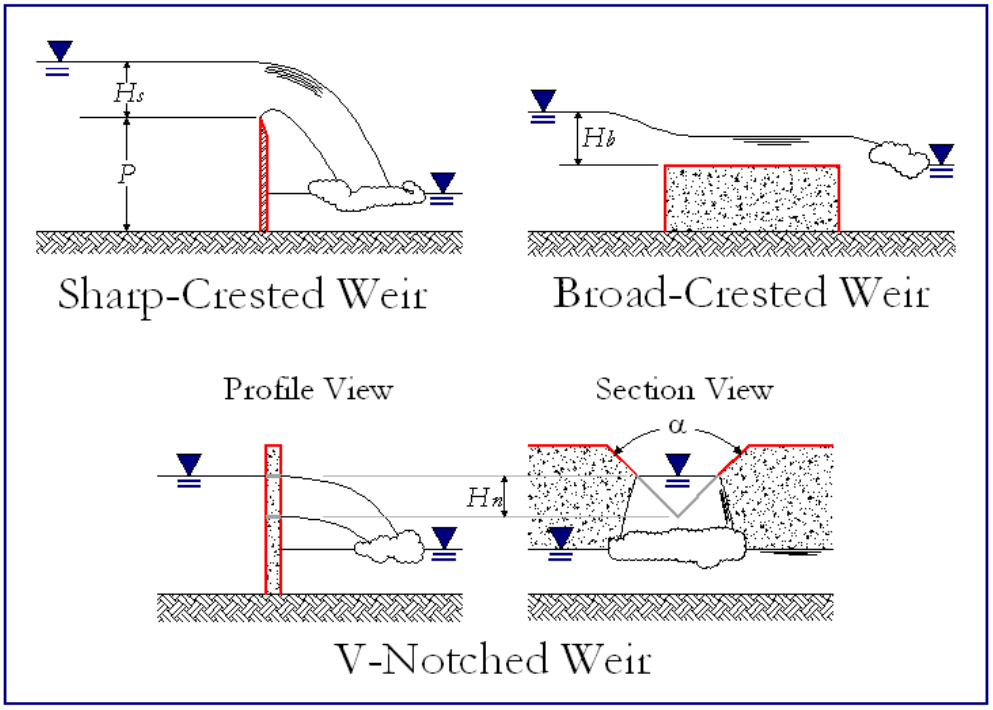

Figure 2-7. Various Types of Weirs.

$$q \propto H^{3/2} \tag{2.22}$$

where $H = H_S, H_b$ or H_n is the height above the given weir structure. The proportionality of Equation 2.22 is converted into an equality by introducing a discharge coefficient unique to each of the weir configurations as described by Henderson (1968). Measurement of flow over weirs is considered to be accurate to within $\pm 3\%$ of the actual discharge (Henderson, 1968) if the weir is properly maintained. However, the utilization of a weir is of significantly larger capital cost that the field deployment techniques discussed previously. There are also regulatory restrictions in many parts of the world that prohibit the construction of weirs as they frequently pose barriers to aquatic species migration.

2.2 Project Economics

The cost of carrying out a hydraulic analysis of a watercourse depends upon a number of factors. For example, the geographical site location (due to remoteness, and varying consulting and construction rates), the resources that are available (both equipment and knowledgeable people), risk involved if the project is not carried out at all, among other factors. It is not the intention of this study to examine all of these factors and how they relate to project economics, but rather examine how resources can be better allocated in a water course project such that the outcome from the hydraulic model is of optimum quality.

With respect to the economics involved in creating a hydraulic model, Reich and Paz (2008) offer a set of general questions that can be adopted into the form:

1. What level of detail is required from the hydraulic model to ensure success for the intended water course project?;
2. What resources are available for the project (i.e. people, funding, equipment, etc.)?;
3. Where should those resources be concentrated?, and;
4. What is the risk involved with a project that is carried out based on the previous three question?

When the relationship between project economics and sensitivity of data quality and quantity are considered, the third question gains the highest priority. To answer this question, an understanding of how field data density and accuracy – either increasing or decreasing – affect a hydraulic model's output results must be attained. The trend that accompanies the relationship between resource investment and project quality as offered by Reich and Paz (2008) is one of asymptotic behavior (Figure 2-8) where the quality of the project does not increase substantially

after a certain point with additional human resource or equipment investment. Reich and Paz (2008) also found a similar relationship where the initial stages of investment take on a project specific relationship.

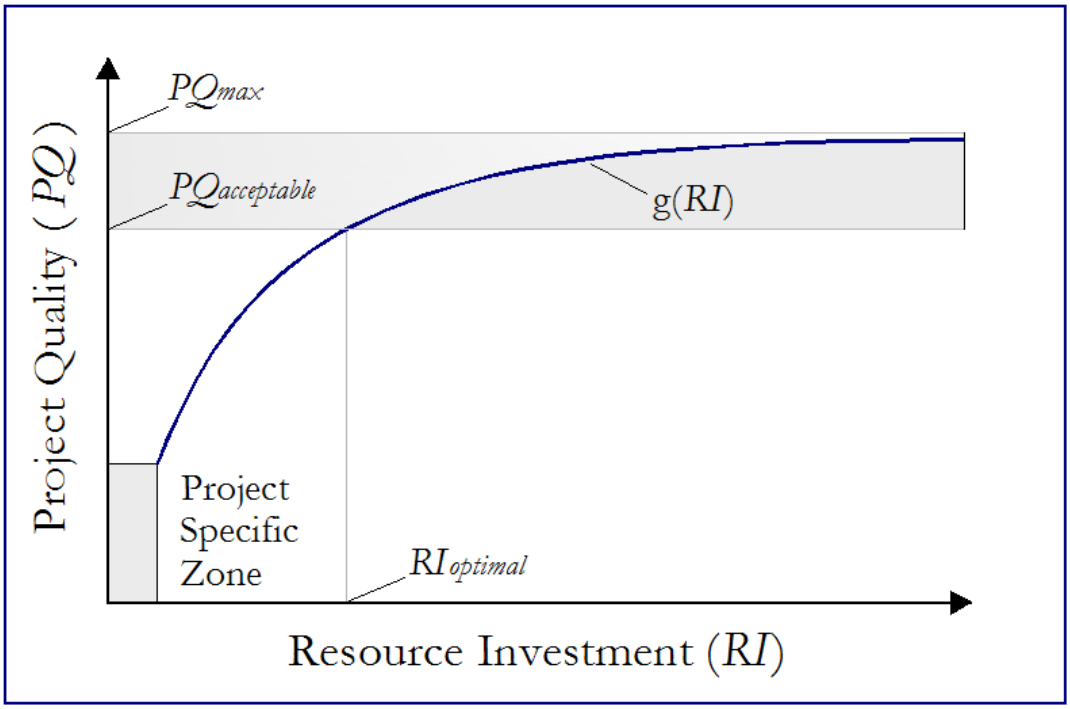

Figure 2-8. Project Quality vs. Resource Investment Relationship.

As illustrated in Figure 2-8, the initial stages of project investment affect a project's quality differently depending on the specifics of the particular project. However, the commonality that exists across projects is the asymptotic function, shown as g(*RI*), which reaches some acceptable level of quality (i.e. $PQ_{acceptable}$) that satisfies the requirements of a project. Investing resources beyond this point would constitute a case of over design.

The definition of resources for a project may include time, money, and equipment, among others. The one common resource definition to all watercourse projects is the approximate human resource hours required to carry out certain tasks. For this reason, the sensitivity of data's quality and quantity will be evaluated from the perspective of where resources (i.e. human resource hours)

should be concentrated to provide the most accurate hydraulic model for a given project economic structure.

CHAPTER 3. METHODS

Given that principle parameters governing the water surface elevation for various flow conditions are functions of slope, cross-sectional geometry and roughness, sites were canvassed for data acquisition that ranged from low gradient (approaching estuarine environments) to steep mountainous channels. Red Hill Creek, located in southern Ontario, Canada (Figure 3-1), which has been intensively studied (WRIS, 2002; Annable et al., in preparation) as an urban restoration project was selected for the entire range of slope of interest, varying channel geometry and bed material roughness. The channel can be represented by one entire reach with slopes ranging between 3.4% and 0.2% over a 7.6km distance (Figure 3-2) or can easily be stratified into three different sub reaches, to evaluate the differences in data accuracy with varying slope conditions.

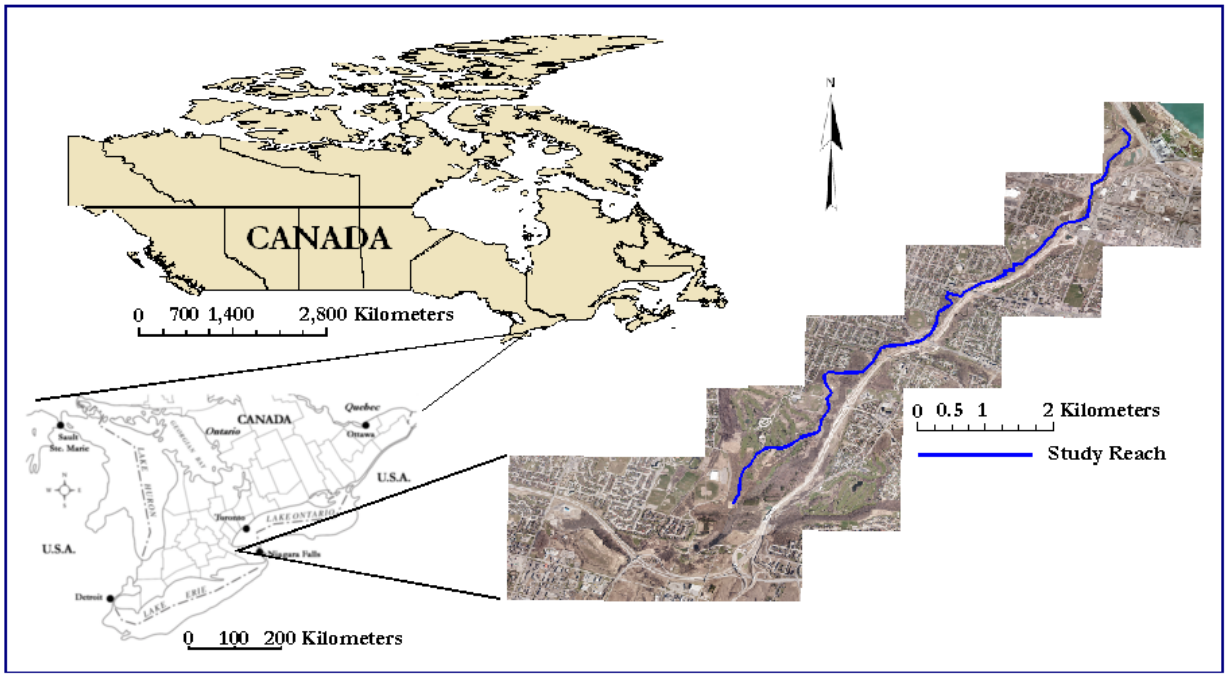

Figure 3-1. Map of Study Site.

The study site is defined by a 23km^2 watershed at the upper limit of the study reach which increases to 78 km^2 at the lower limit of the 7.8km reach from the confluencing of Davis Creek

immediately upstream of King St (Figure 3-2). Upstream of the study reach, the watershed is bisected by the Niagara Escarpment which results in a 25m waterfall and a net relief of 40m over a 1.5km distance terminating at the beginning of the study reach. The watershed is principally comprised of the Halton Clay plain till (Chapman and Putnam, 1984) which is an over consolidated clay deposit with small fractions of angular shale gravels. In several sections along the study reach Queenston Shale outcrops along the bed and banks of the channel which is comprised of red and grey shale with local grey-green shale and interbeds of calcareous sandstone (Brogly et al., 1998). The upper sections of the channel immediately downstream of vertical relief from the Niagara Escarpment are comprised of angular colluvial material ranging in size between small gravels to large cobbles with a remaining matrix of clay. The lower terminus of the study site is comprised of estuarine deposits derived from the watershed and beach sand deposits from long-shore drift processes along the southern limit of Lake Ontario. The combined geology, results in an average bed material particle size of D_{50} = 18.6mm for the entire study reach. The steep and low gradient sub-sections of the study reach range from D_{50} = 128mm to a D_{50} = 0.062mm, respectively. These D_{50} values result in Manning's n coefficients from Equation 2.17 of 0.045 for steep sub-sections and 0.012 for low gradient subsections.

The variation in sinuosity found at the study site is another factor that determines how applicable the results from this study can be applied to other streams. Energy that is dissipated in bends through helical flow and scour in bends is not computationally accounted for in a one-dimensional hydraulic model, so it is important to evaluate reaches with a range in plan form geometry; thus providing results which evaluate a channel with larger bends consistent with riffle-pool channel morphology through straighter channels consistent with step-pool channel morphology. The average sinuosity (Ω) over the entire 7.6km reach is 1.2 but when stratified into steep to mild slope

channel sections (Figure 3-2), the sinuosity ranges between 1.02 and 1.6, respectively. Dimensionless sinuosity is calculated here based on Annable (1996) as follows:

$$\Omega = \frac{L_S}{L_V} = \frac{S_V}{S_O} \quad (3.1)$$

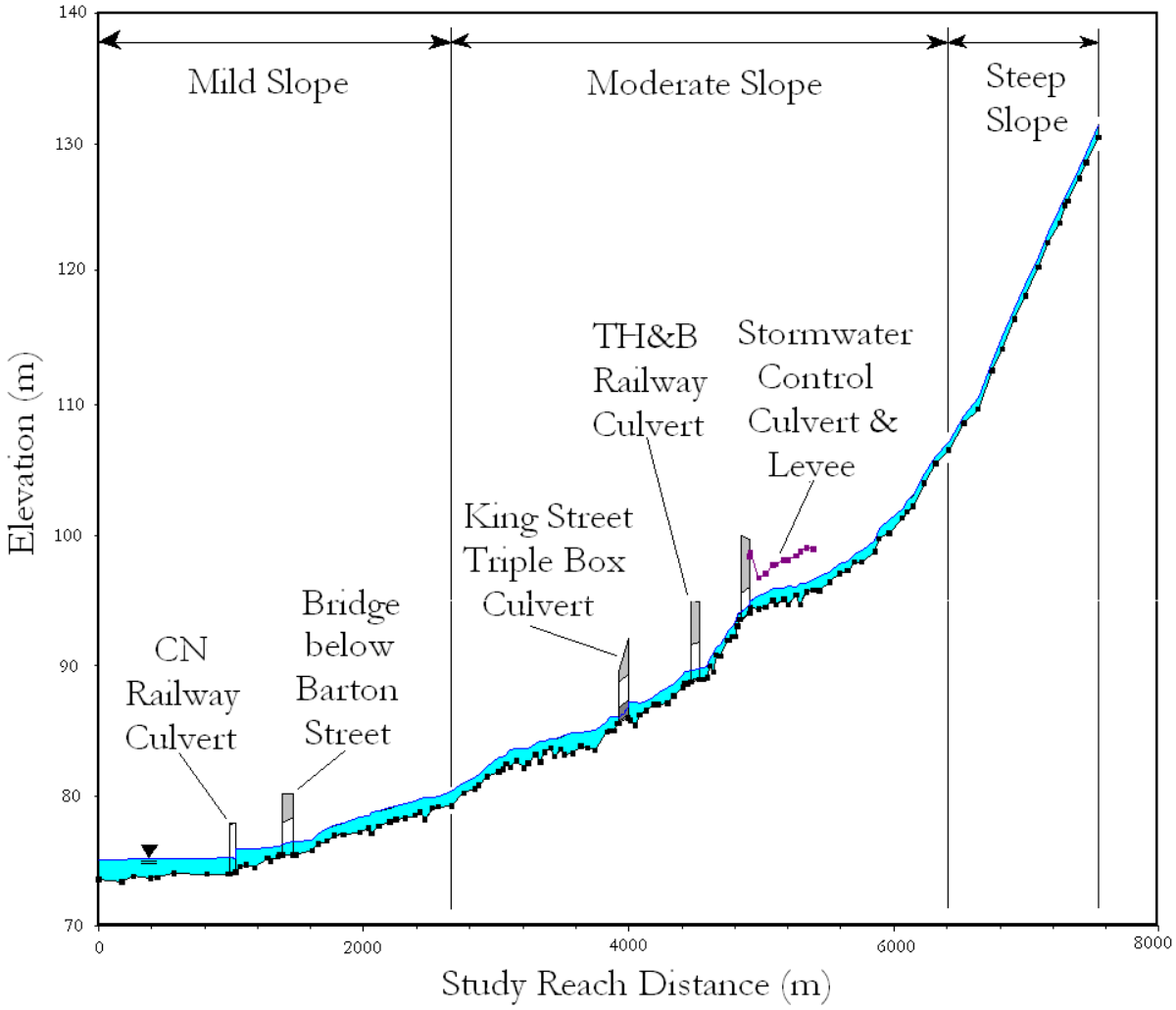

Figure 3-2. Longitudinal Profile of RedHill.

where L_S is the stream length along the bankfull channel centre line, L_V is the length of the valley along the valley trend (L), S_V is the slope of the valley along the valley trend (-) and S_0 is the channel bed slope as previously defined.

The study reach also includes a number of infrastructure elements which include four box culverts, four bridges, an off-line stormwater quantity pond and a series of instream structures to mitigate channel migration and improve fish habitat (Figure 3-3). Energy losses associated with the instream structures and required for proper model calibration are explicitly prescribed based upon pressure transducer data obtained in the field, as described in subsequent sections.

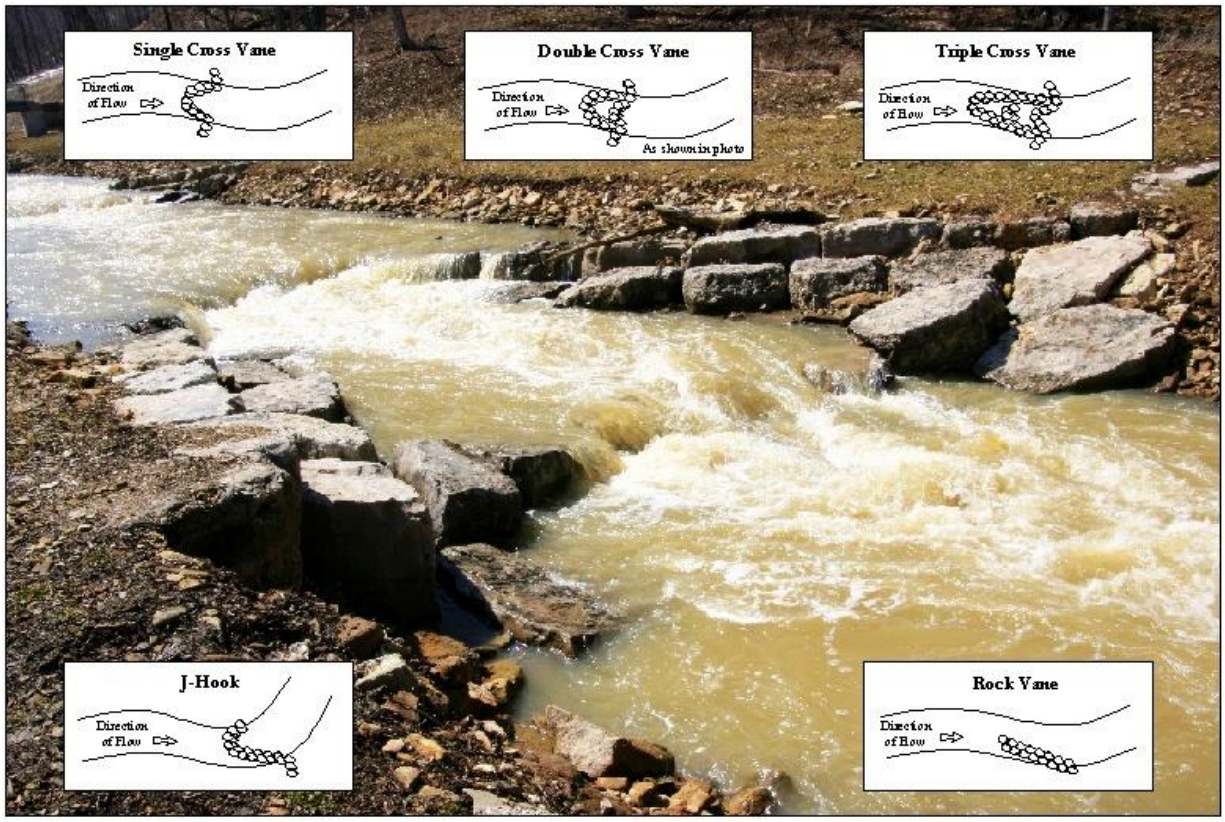

Figure 3-3. Instream Flow Structures.

3.1 Input Data

The objective of this research is to determine an optimal distribution of project resources based upon data quantity, quality and sensitivity for a given study reach. Therefore, the most labour intensive and accurate methods were employed in this study such that lesser levels of resolution and accuracy can be inferred from the findings of this study. In this context, an open transverse

and topographic survey was undertaken of the longitudinal profile of the channel using Sokkia® Set 4E and a Set 5_{30R} total stations. Spatial corrections of the total station surveys were reconciled with a first order Trimble® differential GPS. All data obtained was consistent with the data parameter population requirements of the United States Army Corp's of Engineers program Hec-Ras4b (US Army Corps of Engineers, 2004) which is an North American industry standard for one-dimensional modelling and is used explicitly throughout this research.

As part of the open traverse and topographic study, a longitudinal profile was surveyed of the study reach channel consistent with the methods outlined by Annable (1996). Attributes acquired included the thalweg, left and right bottoms and tops of banks respectively, bankfull stage, flood plain attributes wherever feasible observing significant changes in flood plain slopes, bridges, culverts and instream structures. In the case of infrastructure which may alter the hydraulic conditions in various flood stages, characterizing bridges and culverts were consistent with the methods offered by Haestand (2003) where two cross sections were obtained immediately upstream and downstream of each structure and geometry of each structure obtained. Two standard iron bars (SIB's) were installed and surveyed at a series of locations along the study reach demarcating the left and right limits of cross-sectional surveys that would be undertaken using leveling methods. Each instream structure was also surveyed to capture the specific as-built geometry of each structure. The resulting survey was adjusted to UTM co-ordinates and vertically adjusted to the vertical datum of meters above sea level (MASL). This adjustment was done by reconciling the starting and ending positions of the open traverse with a first-order differential GPS.

The instream structures, illustrated in Figure 3-3, are distributed throughout the study reach to mitigate both vertical and lateral channel migration and dissipate excess stream power (WRIS, 2002). Table 3-1 outlines the quantity and type of structure in each sloped zone.

Table 3-1. Inventory of InStream Structures at Red Hill Creek.

	Single Cross Vanes	Double Cross Vanes	Triple Cross Vanes	J-Hooks	Rock Vanes
Steep Slope Section	0	41	1	0	0
Moderate Slope Section	34	14	3	13	38
Mild Slope Section	14	0	0	3	30

3.1.1 Channel Cross Sections

Permanent benchmarks, as part of the open traverse and topographic surveys, were established at 118 cross sections at an approximate equal distribution throughout the study reach using standard iron bars (SIB's) to characterize the channel and for future erosion surveys. Ten additional cross sections were also surveyed to properly characterize bridges and culverts consistent with the methods outlined by Heasted (2003). Cross-sectional profiles were surveyed between each set of benchmarks using a Sokkia SDL30 Laser level and bar code graduated stadia rod.

Each cross section was oriented perpendicular to the mean average flow direction within the limits of the bankfull channel and perpendicular to the valley trend for flood flow conditions exceeding bankfull discharge. Approximately 20 discrete points were obtained at each cross-section within the limits of the SIB's. Field attributes included, top and bottom of the right and left banks, thalweg, right and left bankfull stage, the elevation at every meter across the channel and any additional notable changes in channel bed transverse slope. The horizontal and vertical positions of each cross-section leveled were transposed and geo-referenced to UTM coordinates and vertically adjusted to MASL datum based upon the coordinates of the SIB' at each cross section.

Where data acquisition was not feasible to collect cross-sectional geometry within the floodplain regions, due to limitations in line-of-sight, using the total station or digital level, the floodplain topography was characterized using a 1m Digital Elevation Model (DEM) of the study region. The longitudinal survey data was combined with the DEM in ArcMap® to derive the valley trend along the study reach. Cross sections were extended beyond the limits of where SIB's were located perpendicular to the valley trend (Annable, 1996). DEM elevations were then extracted into UTM coordinates and post-processed to supplement individual cross-section data measured within the limits of the bankfull channel defined by each left and right sib location. Results of each cross sectional survey are included in Digital Appendix A.

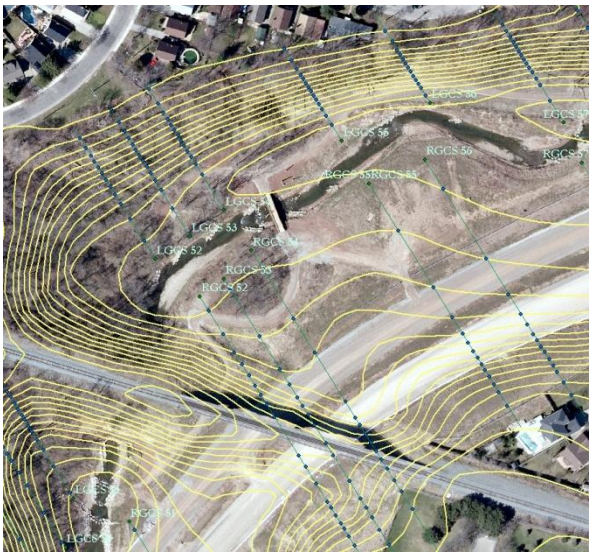

Figure 3-4. Example of 1m DEM and Cross Section Extrapolation Points.

3.1.2 Roughness

Instream channel roughness was parameterized using the grain size analysis results of the Wolman (1954) pebble count method conducted at each cross-section. Particle grain sizes related to the D_{50}, D_{75} and D_{90} percentiles of the frequency distribution were then used in the Strickler equation (Equation 2.18) to compute average cross sectional Manning's n values for each cross-section.

Four methods were used to derive the range of Manning's n values for each cross section. These methods included those developed by V.T. Chow (1959), Anderson et al. (1970), Lane & Carlson (1955), and United States Army Corps of Engineers (1991). The equations used for each of these methods are as follows:

V.T. Chow (1959): $$n = 0.0417\ D_{50}^{1/6} \quad (3.2)$$

Anderson et al. (1970): $$n = 0.0482\ D_{50}^{1/6} \quad (3.3)$$

Lane & Carlson (1955): $$n = 0.0473\ D_{75}^{1/6} \quad (3.4)$$

U.S.A.C.E. (1991): $$n = 0.046\ D_{90}^{1/6} \quad (3.5)$$

Results of the bankfull channel roughness are included in Digital Appendix A. For modelling purposes, an average of the four Manning's n values at each cross section was calculated and used to create the base case model used for result comparisons. At every cross section, the Chow method resulted in the minimum calculated Manning's n value while the U.S.A.C.E. method resulted in the highest calculated Manning's n value. These minimum and maximum values at each cross section were used in evaluating the roughness sensitivity of a hydraulic model as discussed in Section 4.0

For overbank floodplain estimates of roughness (i.e. floodplain and valley walls), the methods offered by Kouwen (1992), also discussed in Section 2.1.2, were employed. In this approach, a visual estimate of vegetation height was taken from field observations at each cross section. These estimates, combined with slope and normal flow depth, were utilized in Kouwen's method to obtain a Darcy-Weisbach friction factor, which was then converted to Manning's n values for

overbank roughness. Results of overbank roughness estimates are included in Digital Appendix A.

3.1.3 Stage & Flow Data

The flow events used for sensitivity analysis were obtained from both field measurements and design flow predictions. The field measurements consisted of two separate flow events, each of which were measured at four different locations along the study reach using the velocity-area method (Buchanan and Somers, 1969) discussed in Section 2.1.3 with an ADP velocity instrument. These flow event measurements are provided in Digital Appendix B. The measured flow events included a base flow scenario and a discharge between base flow and bankfull (referred to as the pre-bankfull event). The pre-bankfull flow event was the highest flow field measurement recorded; therefore, it was used to calibrate the hydraulic model. The model was not calibrated to the base flow scenario.

The bankfull, 20 year, 50 year, and 100 year flow events are also modelled in this study and were obtained from predictions outlined in the City of Hamilton – Philips (2003) and WRIS (2002) and are included in Digital Appendix B. To maintain consistency in modelling and calibrating discharges between field observed and design flow predictions, pressure transducers and field measurements were conducted at locations upstream and downstream of a tributary (Davis Creek confluencing upstream of King St.) and at the upper and lower limits of the study reach.

3.2 Model Scenarios Conditioning

To evaluate model sensitivity, data accuracy and density, a series of numerical experiments were developed to evaluate model performance for varying discharges between base flow and the 100-year flood event. It was considered important to conduct these experiments across a range of discharges as different flows utilize different roughness elements and cross sectional geometry of the channel under varying slope conditions. Six discharge rates were evaluated in the experiments

which included a measured base flow, measured pre-bankfull flow, design bankfull flow, predicted 20-year, predicted 50-year, and predicted 100-year flow events as previously introduced in Section 3.1.4. and summarized in Table 3-2. All flow events utilized a normal depth downstream boundary conditions where the channel slope (S_o) over a series of cross sections remained relatively constant at 0.0001.

Table 3-2. Simulated Discharges.

	Above Davis Creek Confluence (m^3/s)	Below Davis Creek Confluence (m^3/s)	Source / Reference
Base Flow	0.654	1.026	Measured
Pre-Bankfull	2.453	3.038	Measured
Bankfull	10.000	12.000	WRIS (2002)
Predicted 20-Year	57.600	75.600	Philips (2003)
Predicted 50-Year	65.000	87.900	Philips (2003)
Predicted 100-Year	70.600	97.400	Philips (2003)

3.2.1 Calibration

The desired output of a numerical hydraulic model is a result that reflects the field observed conditions in its entirety. However, such representations are not typically achieved without model calibration. Hydraulic model calibration is the process of adjusting roughness coefficients in the model so as to best approximate the measured WSEs. Initial model predictions of the pre-bankfull event simulated WSEs that were significantly lower than observed WSEs.

In the simplifying assumptions of a one-dimensional hydraulic model, several discrepancies arise leading to model calibration. Examination of the one-dimensional form of the Bernoulli energy equation can be used to rationalize the majority of the simulation discrepancies leading to model calibration:

$$z_1 + y_1 + \alpha_1 \frac{V_1^2}{2g} = z_2 + y_2 + \alpha_2 \frac{V_2^2}{2g} + h_L \quad (3.6)$$

where subscripts 1 and 2 refer to consecutive cross sections, z is the thalweg datum elevation (L), y is the flow depth (L), α is the kinetic energy head correction coefficient (-) arising from the departure of hydrostatic and parallel flow line assumptions, V is the velocity and, h_L are the energy losses (L) between sections due to channel form resistance and any other energy dissipation losses.

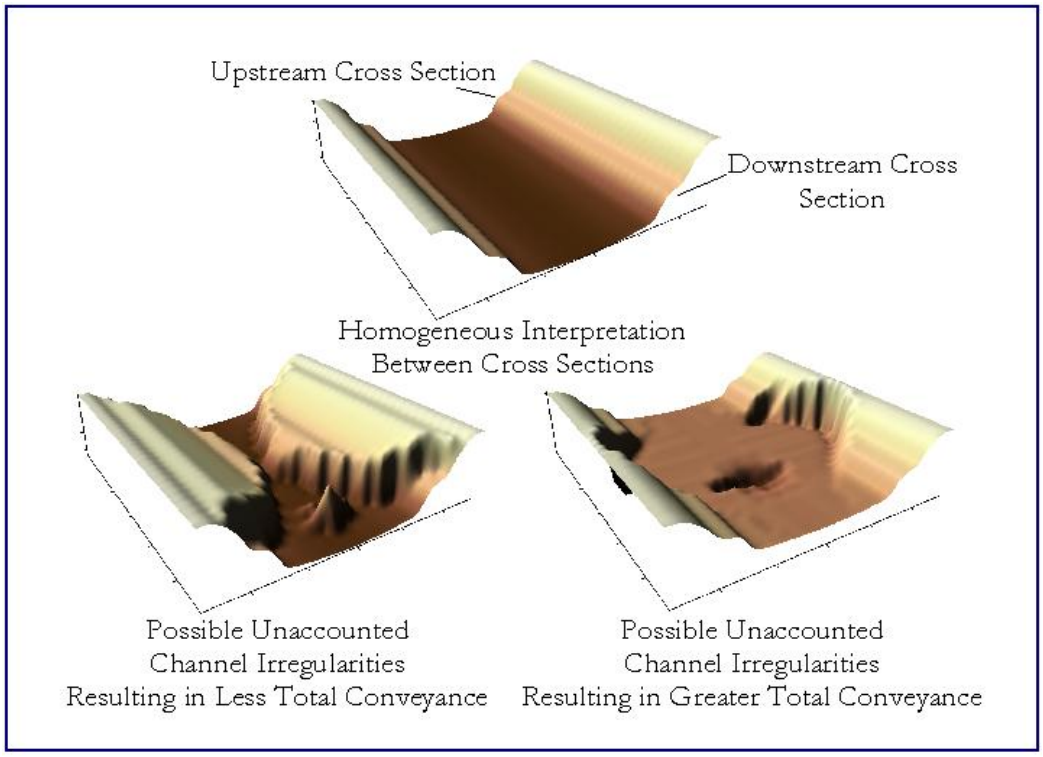

Figure 3-5. Channel Irregularity between Cross Sections.

When the above equation is examined from the perspective of where error could manifest itself to produce an incorrect calculated water surface elevation, the velocity heads ($\alpha V^2/2g$) and energy losses (h_L) contribute to the greatest uncertainty. When the velocity heads are considered, the first

possible reason for an incorrect water surface elevations relates to unaccounted for channel geometry irregularity between cross sections (as illustrated in Figure 3-5). This irregularity would constitute a change in local velocities and conveyance (either a positive or negative) resulting in either a decrease or increase in the adjacent WSE values. This issue is considered relatively small as the field discretization of cross section frequency would have identified and adequately characterized any major geometry discrepancies in the field.

A second reason for discrepancies in the observed vs. simulated WSE's is from unaccounted for differences in roughness between cross sections. As discussed, roughness is accounted for in the Manning's n values entered at each cross section. If these roughness values do not reflect what is actually in the field between cross sections, the measured water surface elevation will differ from the water surface elevation produced by the model.

Table 3-3. Differences between Measured & Calculated Water Surface Elevations for the Measured Prebankfull Flow Event.

*	Measured Water Surface Elevation (m)	Uncalibrated Water Surface Elevation (m)	Difference Attributable to Losses (m)
Steep Slope Section	105.9600	105.76000	0.2000
Moderate Slope Section	89.2486	89.0800	0.1686
Mild Slope Section	77.1631	77.1200	0.0431

* The values presented in this table are for a specific measurement point location in the listed sloped sections.

Likely the largest discrepancies between observed vs. predicted WSE's are derived from energy losses due to instream flow structures and secondary flow in bends. These losses are difficult to include explicitly in the model because they do not occur in the same location as cross sections and are beyond the limits of this study to quantify. Table 3-3 lists the differences between the actual WSE's measured in the field with those of the calculated water surface elevation produced by the uncalibrated model.

When the results of Table 3-3 are combined with the number of structures in each slope classification, a head loss per structure drop[2] of 2.35 mm occurs in the steep slope section, 2.01 mm occurs in the moderate slope section, and 2.54 mm occurs in the mild slope section. This equates to an average energy loss of 2.3 mm for every structure drop. These losses are considered for the measured prebankfull flow condition and therefore not reflective of the entire bankfull roughness or for that matter the roughness associated with the lager flow events considered (i.e. 20 Year, 50 Year, and 100 Year flow events), which would in turn result in larger energy losses. When the average energy loss per structure for the measured prebankfull flow condition is compared to theoretical results obtained from the relative energy loss equation for hydraulic jumps (United States Department of Interior – Bureau of Reclamation, 1984):

$$\frac{\Delta E}{E_1} = \frac{8F_1^4 + 20F_1^2 - (8F_1^2 + 1)^{3/2} - 1}{8F_1^2(2 + F_1^2)} \tag{3.7}$$

where ΔE is the change in specific energy (L) between an upstream and downstream cross sections, E_1 is the specific energy head (L) at the upstream location where $E_1 = y_1 + v_1^2/2g$, and F_1 is the Froude number (-) at the upstream location, the energy losses caused by instream structures at the study site are consistent with energy losses due to weak hydraulic jumps.

The principle model parameter used in hydraulic model calibration is roughness. Manning's n coefficients were only adjusted for the limits of the bankfull channel. No adjustments were made to flood plain roughness parameters as no measured WSE data were sampled under flood flow conditions. Manning's n values for each sloped zone were multiplied by a scaling factor to increase the roughness values such that observed and simulated WSE's were in agreement. These

[2] A structure drop is equal to one spill over in a flow deflector; therefore single cross vanes and j-hooks have 1 structure drop, a double cross vane has 2 structure drops, and a triple cross vane has 3 structure drops.

constants varied depending on the type of sensitivity test being carried out (i.e. raw roughness values used in the model) and are detailed in Table 3-4 below.

Table 3-4. Calibrating Constants applied to Roughness Values.

	Calibration Constants		
	Average Manning's n Simulations	High Manning's n Simulations	Low Manning's n Simulations
Steep Slope Section	2.65	3.16	5.02
Moderate Slope Section	2.55	2.40	3.29
Mild Slope Section	1.12	1.08	1.40

3.3 Numerical Modelling Experiment Constructs

A series of numerical modelling experiments were developed to evaluate how change in data accuracy and density impact model predictions. Data accuracy and density changes include topography (related to survey density or common survey errors), roughness (related to estimation methods), and flow data (related to measurement techniques) to quantify their effects. Each modelling experiment consisted of simulating 1,000 realizations of WSE based on a Monte Carlo sampling of the data accuracy and/or density factor of interest. Within each modelling experiment, these 1,000 realizations represent the WSEs that 1,000 independent hydraulic modellers under the same resource constraints could have predicted. This range of WSEs reflects the fact that there are several different approaches to embarking upon a hydraulic study and survey of a river channel. Each modelling experiment is repeated for a range of available resource constraints. To understand how these realizations were sampled and then compared, the following sub-sections explain both the approach and experiments used throughout this study.

3.3.1 Comparable Axioms

To study the effects of data quality and quantity on a one-dimensional hydraulic model, a number of standard conditions must be established. This will allow the series of results to be quantified

and compared by contrasting the output results from each realization with established standards. These established standards are referred to as axioms from this point forward and a total of three axioms will serve as the foundation of comparison for this study, with the WSE of the second and third axioms being directly compared to uncalibrated and calibrated results, respectively.

The first axiom is the natural condition that exists at the site under measured flow conditions. Since this is the observed behavior of the stream it is what the calibrated model results are attempting to represent for a given level of input data. This axiom serves as a comparison for calibrating the model and for determining the magnitude of the unaccounted for losses as detailed previously in Table 3-3.

The second axiom is the uncalibrated hydraulic model. This axiom is obtained by developing the hydraulic model with the complete set of very intensive field data collected for this study and assuming average Manning's n values without calibration for the channel and overbank areas. Specifically, the second axiom is the resulting model predicted WSE at all 128 cross sections in the study. When various uncalibrated realizations are simulated and compared to this axiom, the degree of data sensitivity can be quantified from the results. This axiom was important in providing relative comparisons for data quality and density for various discharge scenarios where field surveyed WSE's were not available. Therefore, this is an important axiom of comparison for discharges greater than or equal to bankfull discharge.

The third axiom is the calibrated hydraulic model. This axiom is the same in all respects to the second axiom except that the Manning's n values in the model are adjusted according to the calibration factors outlined in Table 3-4. Again, the calibrated Manning's n values produce WSEs that are as close as possible to what was measured in the field for the measured prebankfull flow event conditions. The majority of results in Chapter 4 are focused on the second and third

axioms. It should also be noted the main comparative variable for every sensitivity test in this study is a difference in WSEs between realizations with that of the second and third axiom.

3.3.2 Variance Reduction Approach

In developing the sampling experiments used to perform the various sensitivity tests, a number of sampling strategies were considered. To ensure the precision of results followed a consistent method of comparison that could be quantified progressively towards decreasing error, a variance reduction correlated sampling approach was employed.

Correlated sampling is a variance reduction technique for Monte Carlo studies (Tung et al., 2006) that is particularly suited to the data density investigations considered in this study. This approach ensures that the memory of sampling from the previous realization is included in the expanding pattern of sampling of subsequent realizations. This for example would be consistent with how a hydraulic modeller would select the frequency and distribution of cross sections in the field to develop a hydraulic model. A primary issue is then for the given hydraulic conditions, how many cross sections and at what distribution provides the best result. For example, if a cross section sampling population consists of:

$$\text{Sampling Population - } \{XSec_1, XSec_2, XSec_3, XSec_4, XSec_5, \dots, XSec_j\} \quad (3.8)$$

where XSEC is a given cross section location, and the first realization is conducted using two samples from the population as:

$$\text{First Realization - } f(XSec_1, XSec_4). \quad (3.9)$$

The second realization, which uses additional samples from population (Equation 3.9), may progress in a sampling fashion such as:

$$\text{Second Realization - } f(XSec_1, XSec_4, XSec_2, XSec_5) \quad (3.10)$$

This technique ensures that the results of a realization include the results from previous realizations; hence, in the case of realizations progressing towards a predefined axiom, the variance in realizations continually decreases.

3.3.3 Simulation Experiment Considerations

The simulation experiments developed were consistent with common field data sampling, data density, and data accuracy questions facing hydraulic modellers at the start of a modelling project. Experiments consisted of varying the cross section frequency, cross section discretization, topographic uncertainty in survey methods, and roughness uncertainty. The development of experiment specific code was required to carry out each sensitivity analysis. All codes were programmed using Microsoft® Visual Basic 2005 under the .NET Framework to generate each realization for data input into HEC-RAS4b. Custom post-processing code was also developed for the comparison of each of the realizations to the particular axioms of relevance.

3.3.3.1 Cross Sectional Frequency

When a hydraulic modeller first begins a water course project that involves hydraulic modelling, decisions regarding the location and frequency of cross sections along a study site are required to ensure a satisfactory hydraulic representation (at different discharges) is achieved. This numerical experiment, aside from being the most widely used in this study, looks at the change in model prediction quality as the number of cross sections used to construct the model changes. Again, model prediction quality is measured relative to the three different axioms. As previously mentioned, there are 118 measured cross sections along the natural characteristics of the channel over a 7.6km reach and an additional 10 cross sections included to define the structural geometry of bridges and culverts. Of the 128 total cross sections, 26 are mandatory for defining boundary conditions and therefore it is assumed that a typical hydraulic expert would survey each of these 26 locations. The 26 cross sections include the first and last cross section in the study reach, four

cross sections located at the flow measurement locations along the study reach, and two cross sections immediately upstream and the two cross sections immediately downstream of the five bridges or culverts.

After surveying the above 26 locations, a hydraulic expert must determine where and how many more cross sectional surveys to take. If 10 more cross sections were possible in the project budget, one expert might sample one set of locations while another independent expert might sample a second set of locations. This experiment is constructed to represent this reality by randomly sampling different sets of cross section locations such that experiment results are effectively integrated over a large sample of experts. Random sampling of the remaining 102 cross sections was undertaken in a fashion that housed some implied hydraulic expert logic in the randomization.

The cross section sampling algorithm is described by the example in Figure 3-6. The sampling algorithm returns a single cross section location that is not yet sampled. After an initial sampling scenario has been conducted (e.g. Figure 3.6a), the sampling algorithm would randomly sample one cross section from all potential cross section locations within the longest gap (Figure 3.6b). An additional condition was stipulated in the largest gap protocol such that a buffer zone on each end of the largest gap was included. The buffer ensured that the next randomly selected cross section did not bias either end of the largest gap. The buffer zone was set at 18.5% of the largest gap distance and selected as the smallest buffer zone that would not interfere with boundary conditions and was also based upon the total density of cross section spacing.

It is worth noting that the cross section discretization analysis follows the correlated sampling approach (also known as the variance reduction approach) mentioned earlier, where a minimum number of cross sections are initially used to construct the model followed by the addition of

suites of ten randomly selected cross sections. This addition of cross section suites continues until the maximum number of cross sections is selected and simulated.

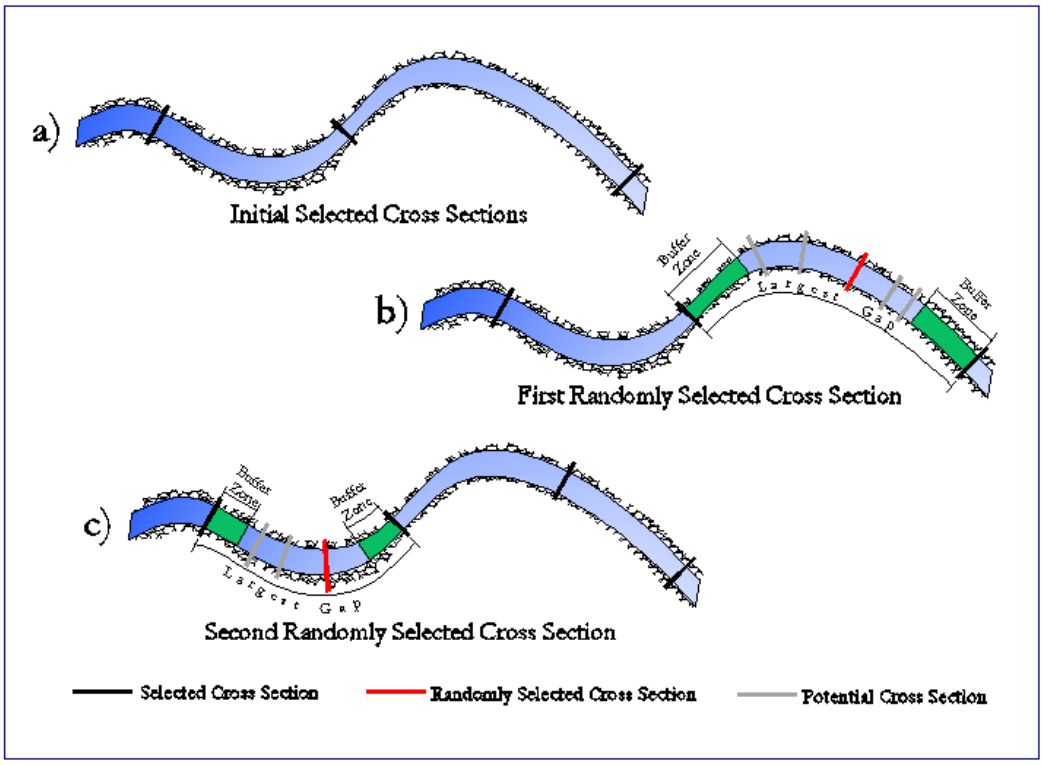

Figure 3-6. Cross Section Selection Method.

3.3.3.2 Minimum Section Discretization

The detail of a cross sectional profile will affect the behavior of the hydraulic model; therefore, a hydraulic modeller must decide how many topographical points to acquire for a given cross section to ensure the best possible hydraulic prediction from the model. The cross sectional profile describes the flood plain geometry and the bankfull channel geometry. The characterization of the channel will also be based upon the discharge range of interest. To quantify the relevance of cross section discretization as it pertains to the main bankfull channel, a numerical experiment was undertaken to compare model predictions with both minimal and very

detailed main channel topographic data at all cross sections. Floodplain geometry was held constant in this experiment.

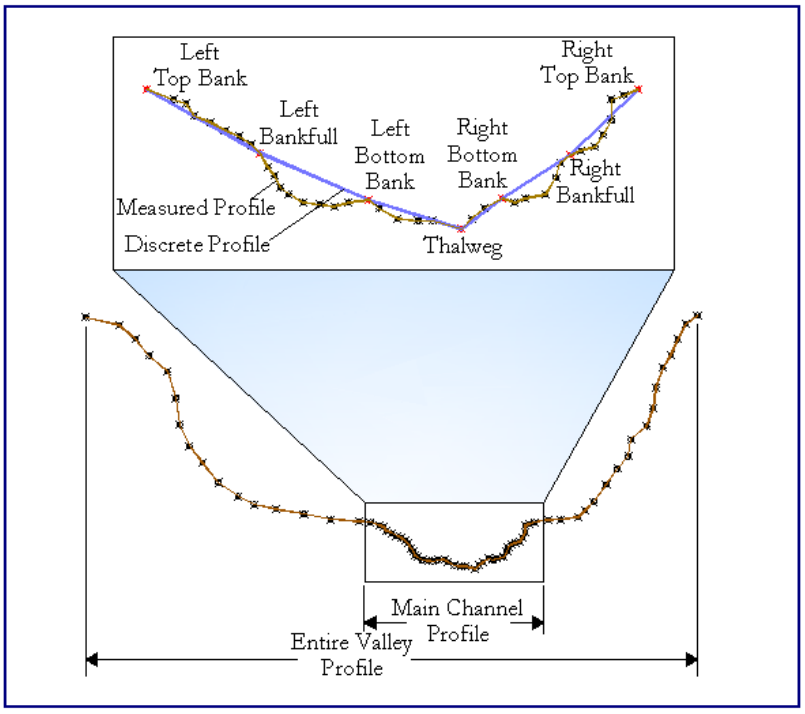

Figure 3-7. Limiting Cross Section Stations.

The minimum detail cross section is defined to include seven mandatory main channel stations which included: left and right top of banks, left and right bankfull elevations, left and right bottom of banks and the channel thalweg. The more detailed cross sections included all additional points in the main channel available from the field data collection process.

Figure 3-7 is an example cross section that contrasts the minimum detail cross section with the completely detailed cross section and is representative of all cross sections in this study in that the detailed cross sections use 5 to 10 times as many points as the minimum detail cross sections.

3.3.3.3 Topographical Uncertainty

A common practice in an open traverse survey is the introduction of *hanger* traverse control points to obtain information beyond the limits of the primary traverse. This commonly occurs in collecting data on river surveys, such as in the characterization of a river bend as illustrated in Figure 3-8. Hangers add an additional potential level of survey error as hanger traverses do not

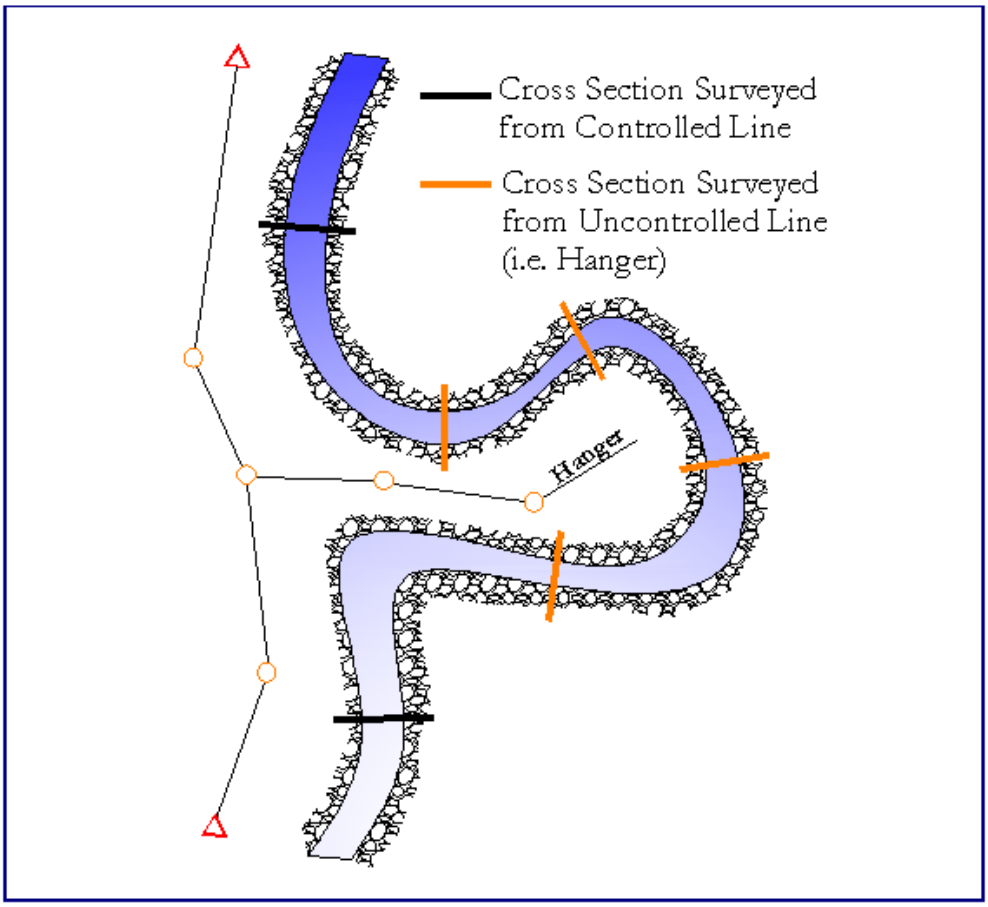

Figure 3-8. Example of a Hanger Traverse and Potentially Impacted Cross Sections.

close back upon their departure control point location. Therefore, cross sections or channel detail obtained from a hanger traverse may propagate localized elevation errors in the topographic survey resulting in a sub-set of cross sections either being characterized by a higher or lower elevation than what exists.

For the study site, it was estimated that an average hanger could affect the topographical data of 3 to 6 consecutive cross sections, based on cross section spacing. To evaluate impact of potential errors associated with a hanger traverse on model predictions, an experiment to simulate the random occurrence of a single hanger error was developed for the case where all 102 potential cross section locations are included in the model. This involved defining the location of the error by randomly sampling one of the potential locations for a hanger (as determined by plan geometry data for the study reach). After a random location is selected, the vertical elevation of a randomly sampled subset of three to six cross sections proximal to the random location is varied. The vertical elevation of each subset is then varied by an error magnitude of -0.20m, -0.10m, -0.05m, -0.025m, 0.025m, 0.05m, 0.10m, or 0.20m.

3.3.3.4 Roughness Uncertainty

The final numerical experiment to evaluate data sensitivity involves the variability of roughness values and how this data effects a hydraulic model prediction that is based on a practitioner's roughness estimations. Depending on the literature reviewed or the field approach employed, roughness can vary in both the main channel and the flood plain. As illustrated in Digital Appendix A, the main channel Manning's n values consistently vary from a minimum possible value calculated via Chow's method to a maximum possible value calculated via the U.S.A.C.E. method. In the case of flood plain roughness, Chow (1959) states that the roughness can vary between approximate Manning's n values of 0.020 and 0.050 depending on the local vegetation.

To investigate variations in estimating channel roughness and the differences in modelling results, a suite of realizations were undertaken which ranged from minimum main channel estimates using Chow's relationship (Equation 3.2) in combination with a multiplier of 0.6 applied to all of the flood plain Manning's n values (calculated using Kouwen's approach). Conversely, to investigate the effects of a high roughness estimation, a suite of simulations were conducted using the highest

calculated main channel Manning's roughness coefficients from the U.S.A.C.E. method (Equation 3.5) in combination with a multiplier of 1.6 applied to all the floodplain Manning's n values (using Kouwen's approach). The WSE's of these results were then compared to previous WSE's numerical experiments that used the mean channel and floodplain roughness to evaluate how important roughness was in predicting WSE for a range of discharges.

CHAPTER 4. ANALYTICS

In order to evaluate the sensitivity results of each numerical experiment, a common comparative error metric was established. Common to all model realizations, and the most important from a flood design perspective, is the water surface elevation (WSE) at each cross section. An error metric referred to as the *Average Absolute Cross Sectional Water Surface Elevation Error* ($\overline{|\in|}$) was calculated for each experiment's results. The calculation of $\overline{|\in|}$ was determined for the uncalibrated (axiom two) or calibrated (axiom three) realizations by:

$$\overline{|\in|} = \frac{\sum_{k=1}^{N} |MWSE_k - WSE_k|}{N} \tag{4.1}$$

where k is the cross section being considered, N is the total number of cross sections in the reach, $MWSE_k$ is the axioms water surface elevation at the cross section being considered[3], and WSE_k is the realization's calculated water surface elevation at the cross section being considered. The error summation is divided by the number of cross sections in the reach to provide a method of comparison between each realization. N is 102 in this study and thus there are 102 MWSE's for each axiom. For realizations with fewer than 102 cross sections, the simulated WSE's are linearly interpolated for MWSE locations with no corresponding cross section in the model. Results can then be plotted to characterize and compare data sensitivity over a range of numerical experiments as illustrated in Figure 4-1.

The box and whisker plot, as illustrated in Figure 4-1, is used extensively throughout this research reporting for its ability to concisely illustrate large quantities of results. Each box and whisker plot included in Figure 4-1 represents 1,000 discrete random realizations for a given number of cross sections in the model (e.g. 10, 20, ...). In the case of outliers where:

[3] This is assumed to be a measureable water surface elevation at the cross section being considered for calibrated realizations.

$$\begin{matrix} \overline{|\epsilon|} > 1.5(upper\ quartile - lower\ quartile) \\ \overline{|\epsilon|} < 1.5(upper\ quartile - lower\ quartile)' \end{matrix} \quad (4.2)$$

results are illustrated as single discrete points. The shaded boxes in each figure represent the calibrated realizations contrasted with axiom three while the unshaded boxes summarize the uncalibrated realizations contrasted with axiom two. Each plot constitutes 22,000 realizations for each numerical experiment for a given discharge of interest.

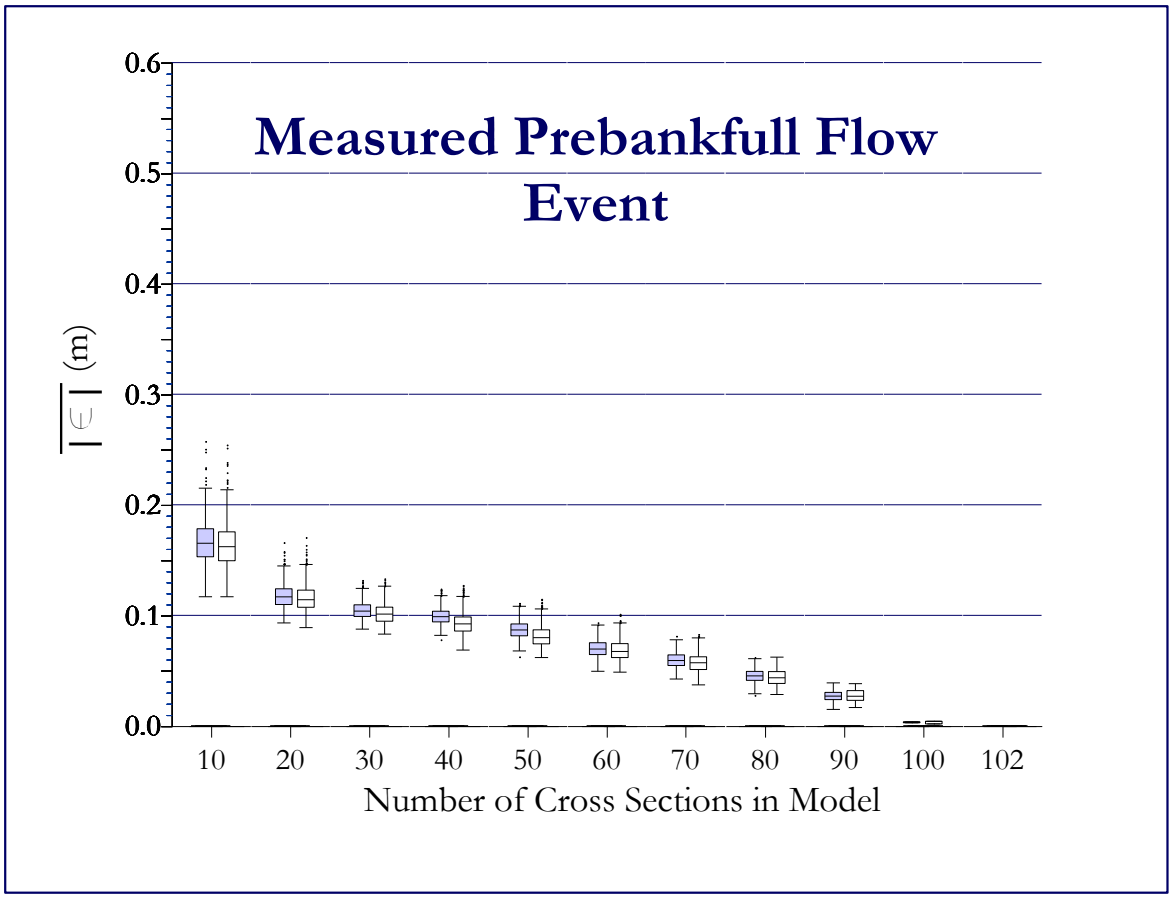

Figure 4-1. Example of comparison between Calibrated & Uncalibrated Results of Absolute Cross Sectional Water Surface Elevation Error.

4.1 Cross Sectional Frequency Results

This first suite of numerical experiments investigated the effects of cross section frequency along the study reach. The 102 cross sections that were available for random sampling ranged in spacing

between 10 meters and 363 meters with an average spacing of 61.23 meters and a standard deviation of $\sigma = 44.75$ meters. The large standard deviation in spacing was the result of more cross sections surveyed in the field along the steeper reach sections compared to the mild and low gradient slope reaches. Six numerical experiments were conducted at discharges ranging from base flow to the predicted 100-year return as outlined in Table 3-2. The average value of Manning's n values for both flood plain and bankfull channels using Equations 3-2 through Equation 3-5 and Equation 2-10 in combination with Equation 2-13. The complete suite of points surveyed in the field was used to define each cross section.

The results of the six numerical experiments are illustrated in Figure 4-2. A general observed trend consist of decreasing absolute error with increasing cross section frequency which would be expected in any numerical method. For the case of 102 randomly added cross sections, this represents the condition of WSE's of axiom two and axiom three, being a full uncalibrated and full calibrated model respectively, which will result in zero absolute error (i.e. the realization that each simulation is being contrasted against). The relative values of absolute error remain relatively consistent for discharges between base flow and the bankfull discharge where only the roughness value associated with the bankfull channel predominates the resistance to flow and thus the final WSE's. When flows exceed bankfull discharge where differences in flood plain roughness combined with different distances between successive cross sections on the flood plain versus the main channel result in larger variability in WSE's, a larger absolute error is observed in all flood flow conditions. Examination of Figure 4-2 also illustrates the case of largest potential error occurring for the 100-year predicted discharge with the least amount of cross sections (10) for both the calibrated and uncalibrated results with absolute errors of $\overline{|\in|} = 0.292m$ and $\overline{|\in|} = 0.339m$ respectively.

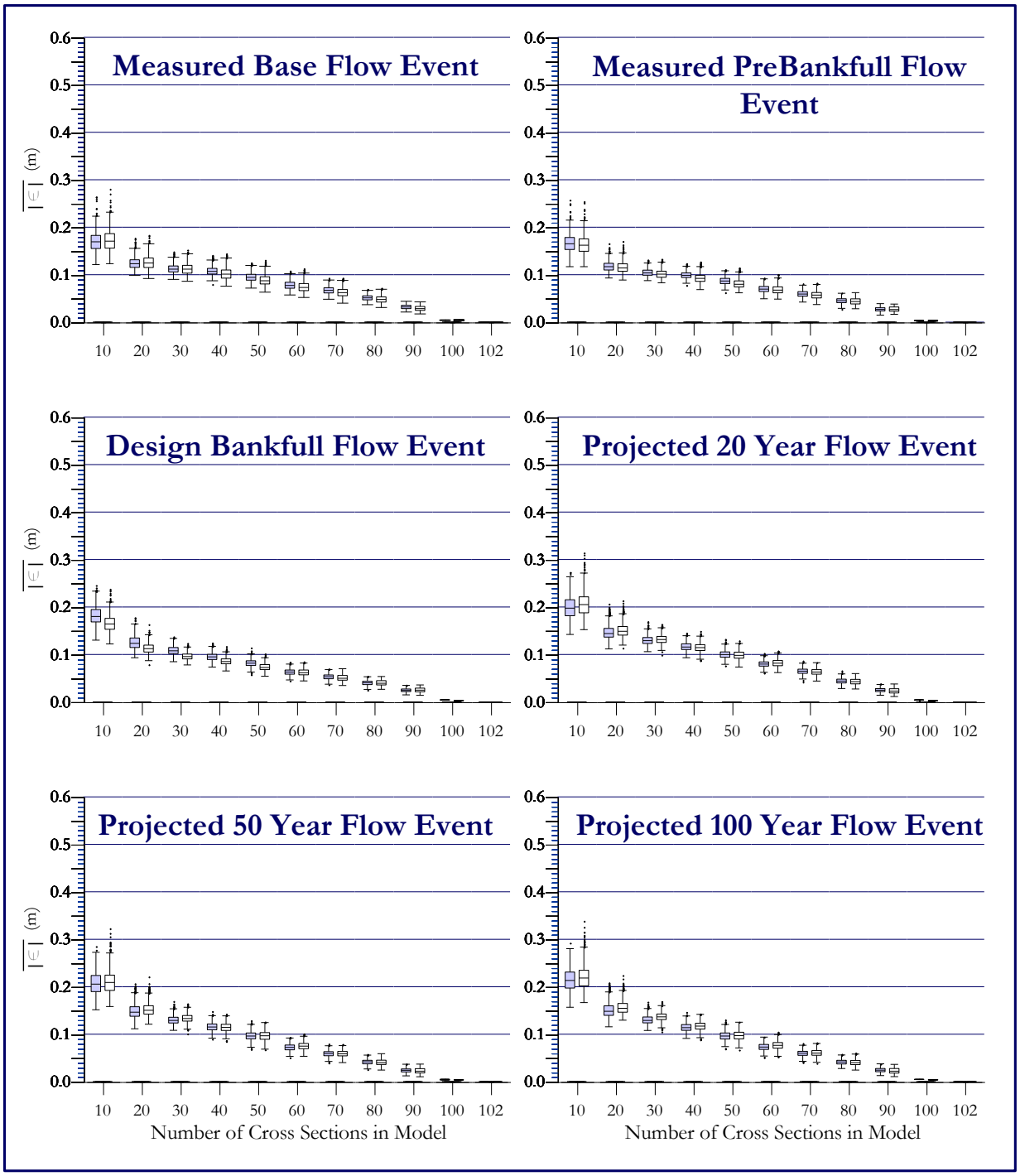

Figure 4-2. Results of Cross Sectional Frequency using Mean Roughness Values and Complete Cross Sectional Detail.

The absolute errors relate to a maximum water surface difference at particular cross sections of 1.33m and 1.99m for the calibrated and uncalibrated experiments respectively. The cross sections

that experience this large error are located in the steep zone along the study reach where the flow passes around a bend.

Upon closer inspection of Figure 4-2 it is noted that there is not a significant reduction in absolute error between 30 – 60 randomly sampled cross sections for flows ranging between base flow and the bankfull conditions. Conversely for discharges greater than bankfull, a relatively constant linear decrease in absolute error occurs with increasing discretization. These results suggest that if a hydraulic modeller is investigating the hydrogeomorphic processes of a channel (within the discharge range up to bankfull) a threshold is achieved within the cross section frequency of the hydraulic model where there will be no appreciable decrease in accuracy with the addition of channel sections unless a high level of cross section frequency is needed (such as for the investigation of sediment transport of bed material). Juxtapose for predicting WSE's in flood flow conditions, the continued addition of cross sections decreases absolute error. Therefore, based upon the sensitivity of a hydraulic model, a number of cross sections can be chosen by a hydraulic modeller to balance model accuracy (i.e. absolute error) and human resources expenses associated with data collection of cross sectional data.

It is also worth noting from examination of Figure 4-2 that the minimum calibrated and uncalibrated absolute error of 10 randomly added cross sections for all discharges is lower than the maximum absolute error of 30 randomly sample cross. These results suggest that depending on how a hydraulic modeller selects the cross section locations, a model with an average cross section spacing of 222 m (i.e. 10 cross section locations) could be more effective than one with an average cross section spacing of 103.7 m (i.e. 30 cross section locations) – roughly half the cross section spacing distance. The challenge in such an observation is that a hydraulic modeller does not know *a priori* the distribution of cross-section spacing and where such cross sections should be measured

in the field to attain the minimum error. This maximum and minimum value comparison between cross section spacings is applicable to other numbers of randomly added cross sections as well; however, the interval between maximum and minimum results decreases as more and more cross sections are added to the model.

To further summarize the results of Figure 4-2, the average of the median $\overline{|\in|}$ for all discharge experiments were calculated for both the calibrated and uncalibrated scenario for each set of randomly added cross sections. Table 4-1 summarizes the findings which demonstrate how closely the calibrated and uncalibrated results resemble each other in this simulation experiment. The slope of the line between the *average of median* $\overline{|\in|}$ *across all flow conditions vs. the average cross section spacing in the model* identifies the increase in accuracy as cross section spacing is increased from one suite of randomly added cross sections to the next (which is also illustrated in Figure 4-3). These results then provide a metric of the increase in WSE accuracy with increasing cross section frequency. For example, if the number of cross sections is increased from 50 to 60, the

Table 4-1. Summary of Cross Section Spacing Results.

Number of Cross Sections Randomly Added to Study Reach	10	20	30	40	50	60	70	80	90	100	102
Average Cross Section Spacing in model (m)	222.2	172.8	141.4	119.6	103.7	91.5	81.9	74.1	67.6	62.2	61.2
Calibrated: Average of Median $\overline{\lvert\in\rvert}$ across all flow conditions (m) *	0.189	0.134	0.118	0.108	0.092	0.072	0.061	0.044	0.026	0.005	0.000
Calibrated: Slope of Average of Median $\overline{\lvert\in\rvert}$ *vs.* Average Cross Section Spacing (m/m)	(-)	0.001	0.001	0.000	0.001	0.002	0.001	0.002	0.003	0.004	0.005
Uncalibrated: Average of Median $\overline{\lvert\in\rvert}$ across all flow conditions (m) *	0.188	0.134	0.118	0.104	0.089	0.072	0.059	0.042	0.025	0.004	0.000
Uncalibrated: Slope of Average of Median $\overline{\lvert\in\rvert}$ *vs.* Average Cross Section Spacing (m/m)	(-)	0.001	0.001	0.001	0.001	0.002	0.001	0.002	0.003	0.004	0.004

* The Average of Median $\overline{|\in|}$ across all flow conditions is calculated by summing each flow event's median for a certain number of added cross sections - calibrated or uncalibrated - and dividing by the number of flow events.
** The slope values are calculated consecutively across the table (i.e. the slope between the 10 and 20 randomly added cross sections is listed below the 20).

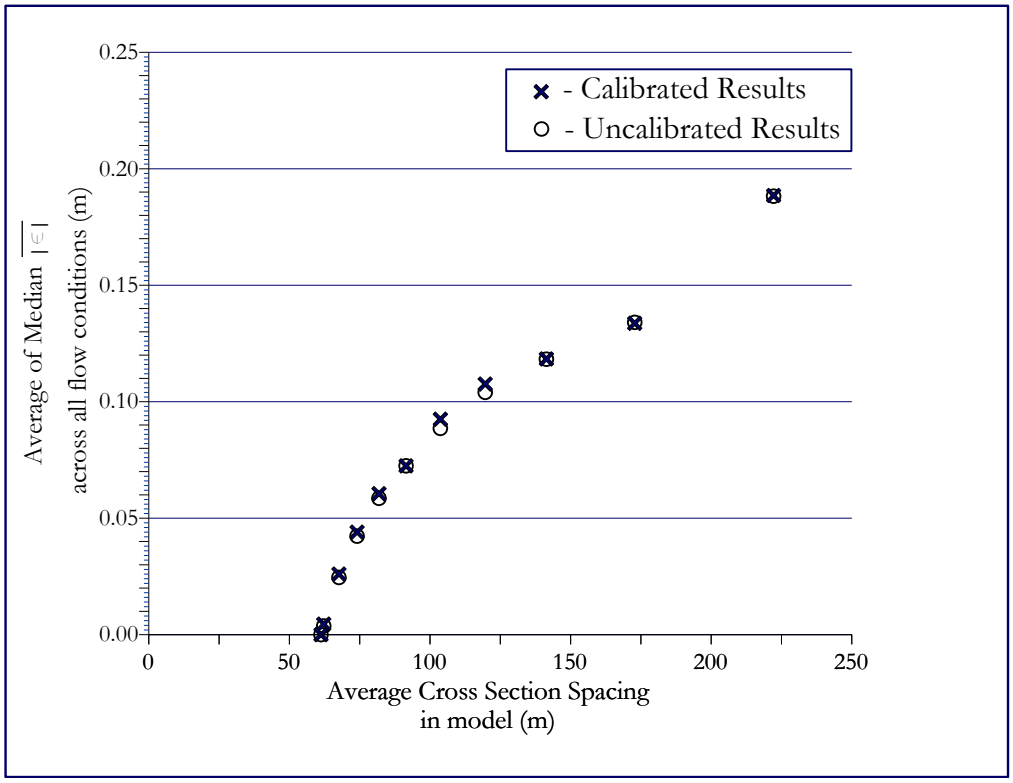

Figure 4-3. Summary of Cross Section Frequency Average of Median $\overline{|\epsilon|}$ for all Flow Events.

slope of the line between these two points is 0.002 m/m for a calibrated scenario; thus achieving an additional 2mm in WSE accuracy for each cross section added. In general, the results show that for every meter in reduction in cross section spacing, a hydraulic modeller can expect between 0mm to 5 mm of increased accuracy of a simulated WSE's. Therefore, based upon regional standards and specified freeboard tolerances, cross section spacing can be estimated to provide an initial estimate of a given reaches cross sectional frequency (excluding cross sections required for boundary conditions).

4.2 Minimum Section Discretization Results

The second suite of numerical experiments evaluated the effects of cross section resolution on the resulting WSE's for the range in discharges previously studied. Realizations conducted for these

experiments were similar to those of Section 4.1 with the only difference being a minimum bankfull channel cross section definition as outlined in Section 3.3.3.2. Discrete points which defined the bankfull channel were limited to: left and right top of banks, left and right bankfull elevations, left and right bottom of banks and the channel thalweg. Comparisons were then made between the results presented in this section and those of Section 4.1 using the full complement of cross section detailing.

In general, the results of Figure 4-4 illustrate similar trends to those of Figure 4-2 for decreasing absolute error with increasing cross section frequency, and also increasing error with increasing discharge. Detailed inspection of Figure 4-4 reveals that realizations considering finer discretization (i.e. more than 80 cross sections in the model), the absolute error does not tend to zero but remains at some residual value of $\overline{|\epsilon|} > 0$ as compared to Figure 4-2. The residual for both the calibrated and uncalibrated experiments represents the absolute error discrepancy when simulating WSE's using minimal vs. detailed cross section resolution. Thus, unless a hydraulic modeller is investigating hydrogeomorphic processes or sediment transport processes, there is no clear benefit in high resolution bankfull channel definition if the minimum number of cross sections to produce WSE' are desired.

To further illustrate the relative significance of bankfull channel resolution, the results of Figure 4-4 are summarized in Table 4-2 and are illustrated in Figure 4-5. Both Table 4-2 and Figure 4-5 demonstrate that the resolution of cross section detailing becomes less important as the spacing between cross sections is increased and that the absolute error attributed to cross section resolution is insignificant compared to cross section frequency. Thus, the absolute error caused by scarcely surveyed cross sections predominates the error or short falls caused by minimal cross section detailing or unaccounted for channel irregularity. A caveat to this interpretation may exist

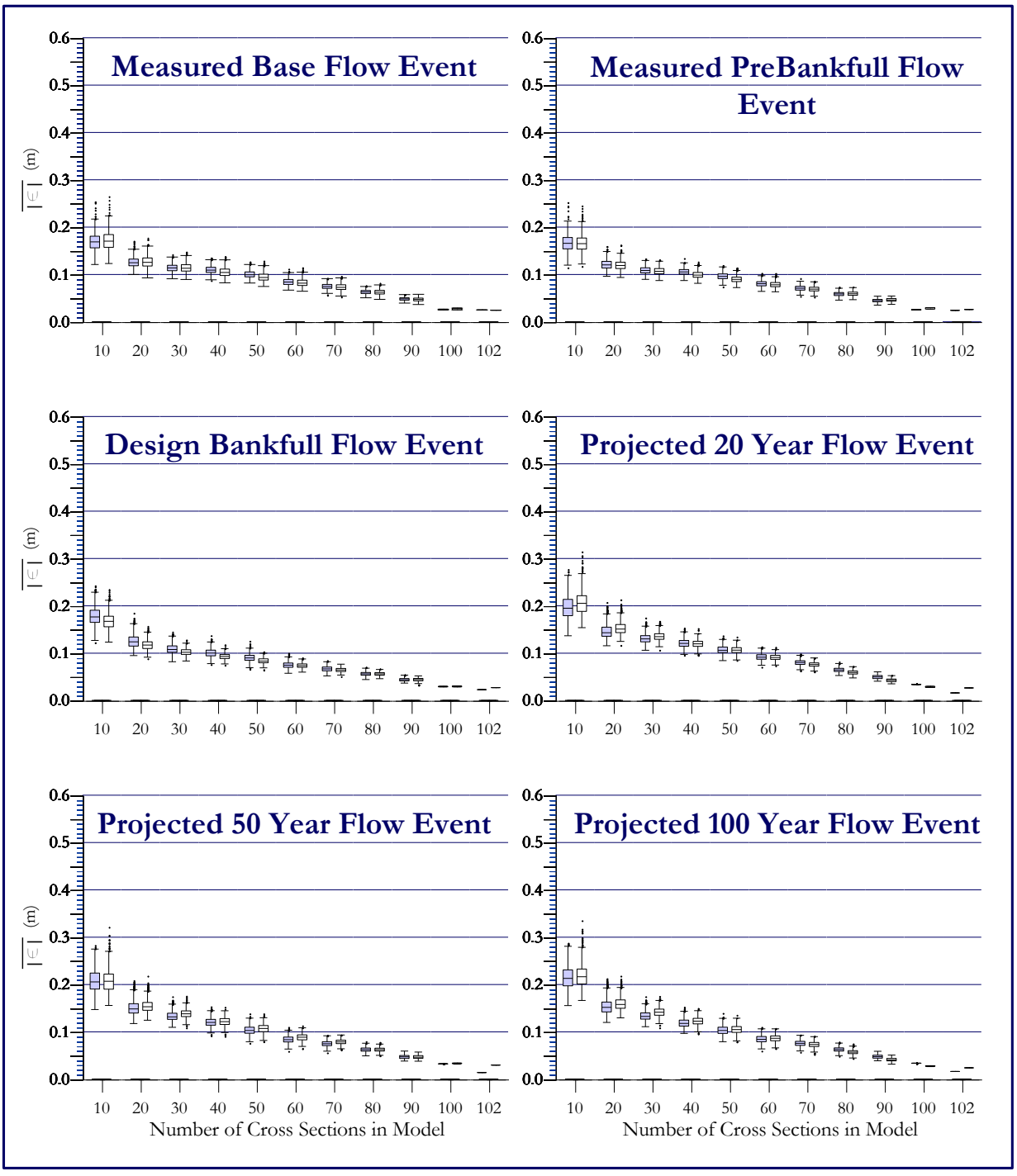

Figure 4-4. Results of Minimum Cross Section Resolution in Conjunction with Cross Section Frequency using Average Roughness Values.

Table 4-2. Difference between Average of Median $\overline{|\in|}$ for Minimum Station Analysis and Cross Sectional Discretization Analysis.

Number of Cross Sections Randomly Added to Study Reach	10	20	30	40	50	60
Average Cross Section Spacing in model (m)	222.2	172.8	141.4	119.6	103.7	91.5
Calibrated: Difference between Average of Median $\overline{\|\in\|}$ across all flow conditions for Minimum Station results and Cross Section Discretization results (m) *	-0.001	0.002	0.002	0.005	0.007	0.011
Uncalibrated: Difference between Average of Median $\overline{\|\in\|}$ across all flow conditions for Minimum Station results and Cross Section Discretization results (m) *	0.000	0.003	0.004	0.006	0.009	0.011
Number of Cross Sections Randomly Added to Study Reach	70	80	90	100	102	
Average Cross Section Spacing in model (m)	81.9	74.1	67.6	62.2	61.2	
Calibrated: Difference between Average of Median $\overline{\|\in\|}$ across all flow conditions for Minimum Station results and Cross Section Discretization results (m) *	0.013	0.017	0.021	0.026	0.020	
Uncalibrated: Difference between Average of Median $\overline{\|\in\|}$ across all flow conditions for Minimum Station results and Cross Section Discretization results (m) *	0.014	0.017	0.020	0.026	0.026	

* The Average of Median $\overline{|\in|}$ across all flow conditions is calculated by summing each flow event's median for a certain number of added cross sections - calibrated or uncalibrated - and dividing by the number of flow events.

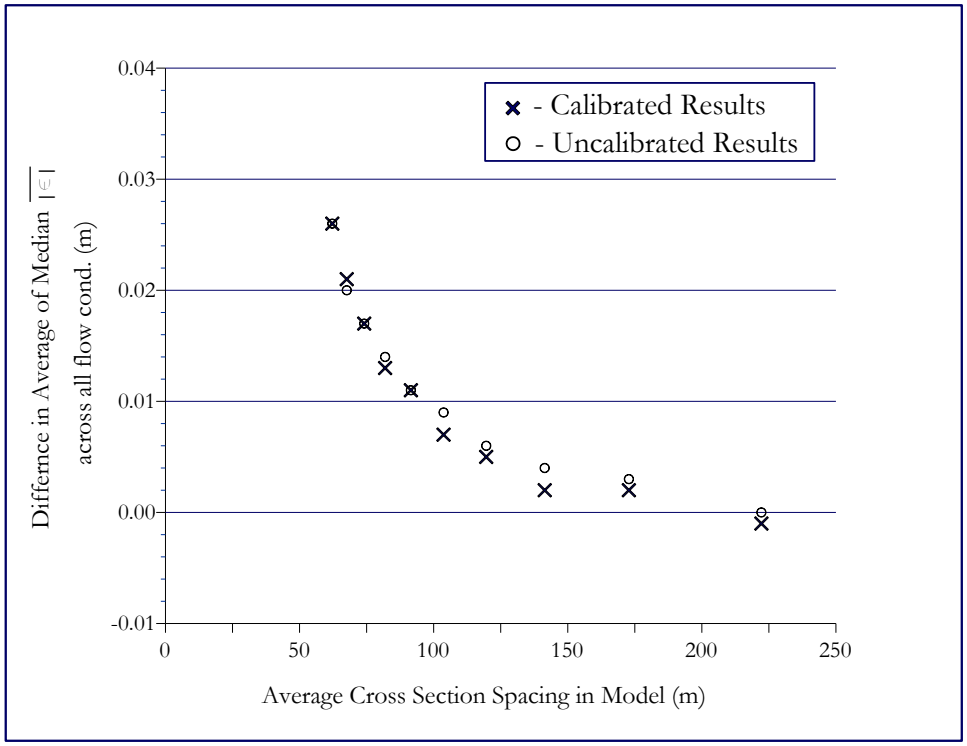

Figure 4-5. Difference between Average of Median $\overline{|\in|}$ for all Flow Conditions for Complete Versus Minimum Cross Section Resolution.

if bedforms are present (such as dunes, anti-dunes etc.), but such features would be considered typically in a sediment transport study where a higher degree of discretization would be required to maintain conservation of mass.

4.3 Topographical Uncertainty Results

The numerical experiments investigated in this section examine the effects of survey error on resulting WSE's. The purposes of these experiments are to evaluate the accuracy of traverse surveys and the resulting absolute error and to relate the level of acceptable error to human resource effort. To investigate errors propagated by a survey traverse, it was considered that vertical discrepancies in traverse control would propagate the largest absolute error in WSE's. Therefore, hangers were investigated that would effect a random number of 3 – 6 clustered cross sections at any random location along the reach of the model. As discussed in Section 3.3.3.3, a series of realizations are conducted down the entire length of the channel randomly selecting any cross section and choosing 2 – 5 cross sections immediately surrounding the randomly selected cross section. The suite of 3 – 6 cross sections were then randomly varied in elevation between -0.20m, -0.10m, -0.05m, -0.025m, 0.025m, 0.05m, 0.10m, and 0.20m. The entire suite of 102 cross sections was utilized in this analysis with the highest cross sectional resolution available for each cross section. The results of these findings are presented in Figure 4-6.

The absolute error effects from these analyses proved to be extremely small, relative to errors associated with cross section discretization or resolution. It is noted in Figure 4-6 that the ordinate axis of all six discharge experiments has been magnified by a factor of 12 to better illustrate the results. The largest absolute error effects are found as an outlier for the calibrated analysis where a hanger of -20 cm elevation discrepancy is into a model for the 100-year flow

event where $\overline{|\in|} = 0.049m$. Similarly, $\overline{|\in|} = 0.026m$ for the uncalibrated experiments where a +20cm vertical discrepancy is introduced.

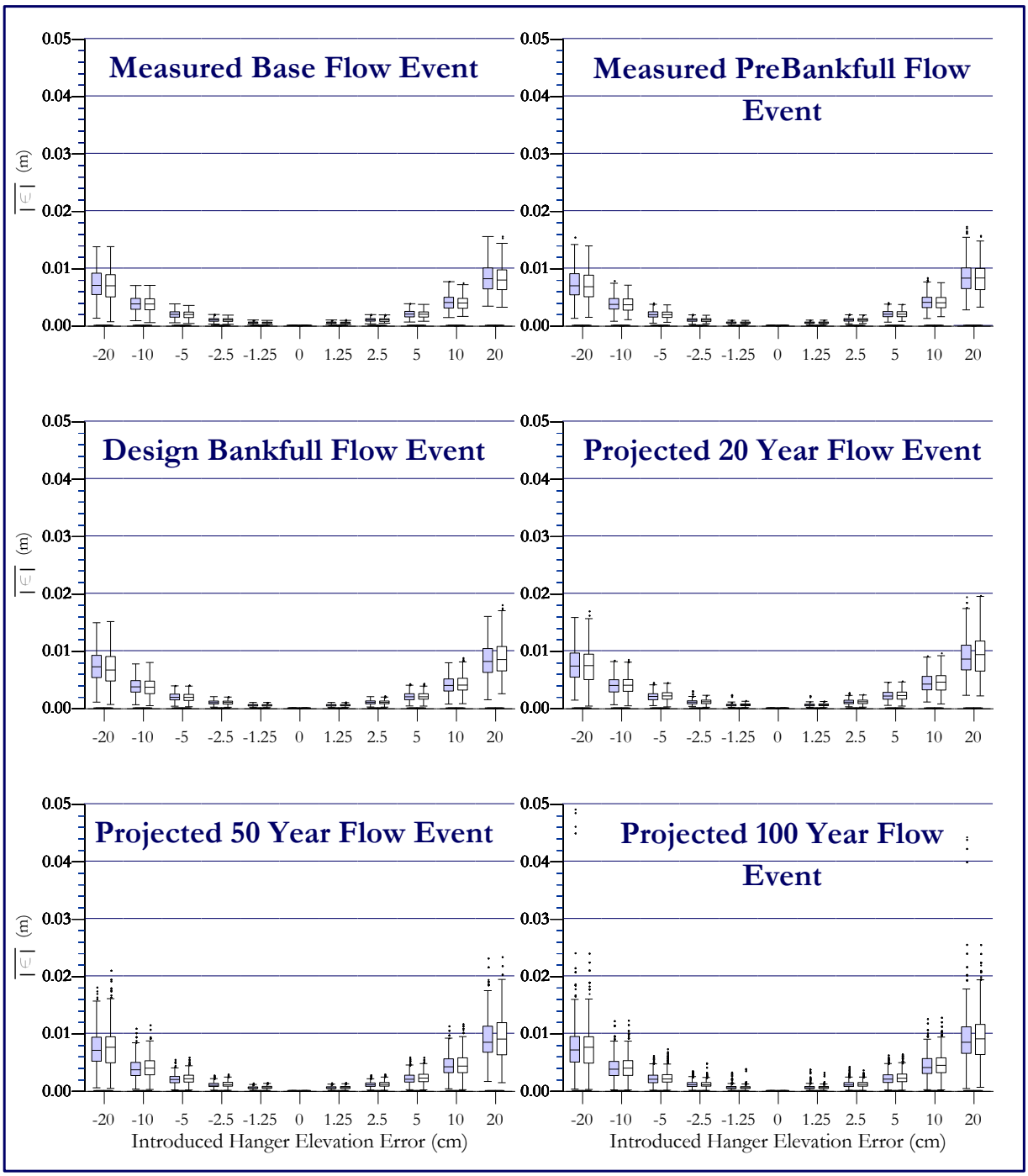

Figure 4-6. Results of Topographical Uncertainty (i.e. hangers) Employing all Cross Sections and Detailed Cross Section Resolution using Average Roughness Values.

Detailed inspection of the results reveals that the largest absolute errors occur in reaches of the channel where a vertical discrepancy in a hanger is in close proximity to infrastructure boundary condition constraints (such as bridge or culverts). For example, the maximum absolute error occurs for a hanger that affects six cross sections in the calibrated axiom which is immediately upstream of a control culvert. In this case, by dropping the hanger's elevation by 20 cm results in a drop in the WSE of 0.89m at one of the cross sections where a backwater profile occurs. Conversely, in reaches distal to any boundary conditions that will not significantly effect the water surface profile beyond the limits of the hanger location (such as infrastructure or boundary conditions), simulated WSE consistently varied in direct correlation to the amount of vertical error introduced. Therefore, as long as the regionally specified freeboard limits are within the error propagated by a hanger, this amount of error could be considered acceptable in the traverse survey order of accuracy.

4.4 Roughness Uncertainty Results

Roughness uncertainty was evaluated for flow conditions ranging between base flow and the 100-year predicted discharge considering both variations in Manning's n values to both the bankfull channel and flood plain at each cross section. Similar to the analysis presented in Section 4.1, the results here included random selection of suites of 10 cross sections ranging in realizations between 10 and 102 sections using the high resolution detail used in each cross section. The relative change in roughness values used in these experiments are outlined in Table 4-3. The first suite of analyses involved investigating the effects of under estimating Manning's n values in both the main channel and floodplains. The results for this analysis are presented in Figure 4-7. These results for discharges equal to or below bankfull discharge demonstrate similar trends to those of Figure 4-2 where only effects of adjusting the main channel roughness coefficient would be experienced. However, where flows exceed bankfull discharge and enter the floodplain, there is a

systematic decrease in absolute error such that at a cross section frequency of $k \approx> 40$ there is no significant decrease in absolute error for the calibrated discharge scenarios regardless of how many additional cross sections are added to the model. In the case of the calibrated 100-year discharge where all 102 cross sections are utilized, an average absolute error of $\overline{|\in|} = 0.144m$ results which relates to water surface error ranging between 0.02cm and 90cm. These results indicate that in acquiring cross sectional information to calculate WSE's, if the water surface elevation of flood flow discharge is of primary importance, characterization of Manning's roughness on the flood plains becomes a more important parameter than cross section discretization to adequately quantify the hydraulic model regardless of the increase in channel cross section frequency.

Table 4-3. Range in Manning n Roughness Estimates for Main Channel and Floodplain Regions with Varying Slope Reaches.

Sub-Reach Slope	Low Manning's n Range		Average Manning's n Range		High Manning's n Range	
	Main Channel	Flood Plain	Main Channel	Flood Plain	Main Channel	Flood Plain
Steep	0.0083 – 0.0264	0.0221 – 0.0431	0.0184 – 0.031	0.0368 – 0.0718	0.0291 – 0.0349	0.0589 – 0.1149
Moderate	0.0083 – 0.0251	0.0083 – 0.0608	0.0117 – 0.0292	0.0138 – 0.1014	0.0196 – 0.0349	0.0221 – 0.1622
Mild	0.0083 – 0.0296	0.0083 – 0.0274	0.0097 – 0.0347	0.0138 – 0.0456	0.0115 – 0.0392	0.0221 – 0.0730

The calibrated results of Figure 4-7 are notably different than those of previous experiments (i.e. Figure 4-2), especially during flow events with levels greater than bankfull. The calibrated results continue to decrease in absolute error until a minimum value of $\overline{|\in|} = 0.068m$ is achieved utilizing all 102 available cross sections. The WSE's errors associated with minimum roughness estimates ranged between 0.02cm and 41cm. It is further worth noting that the maximum

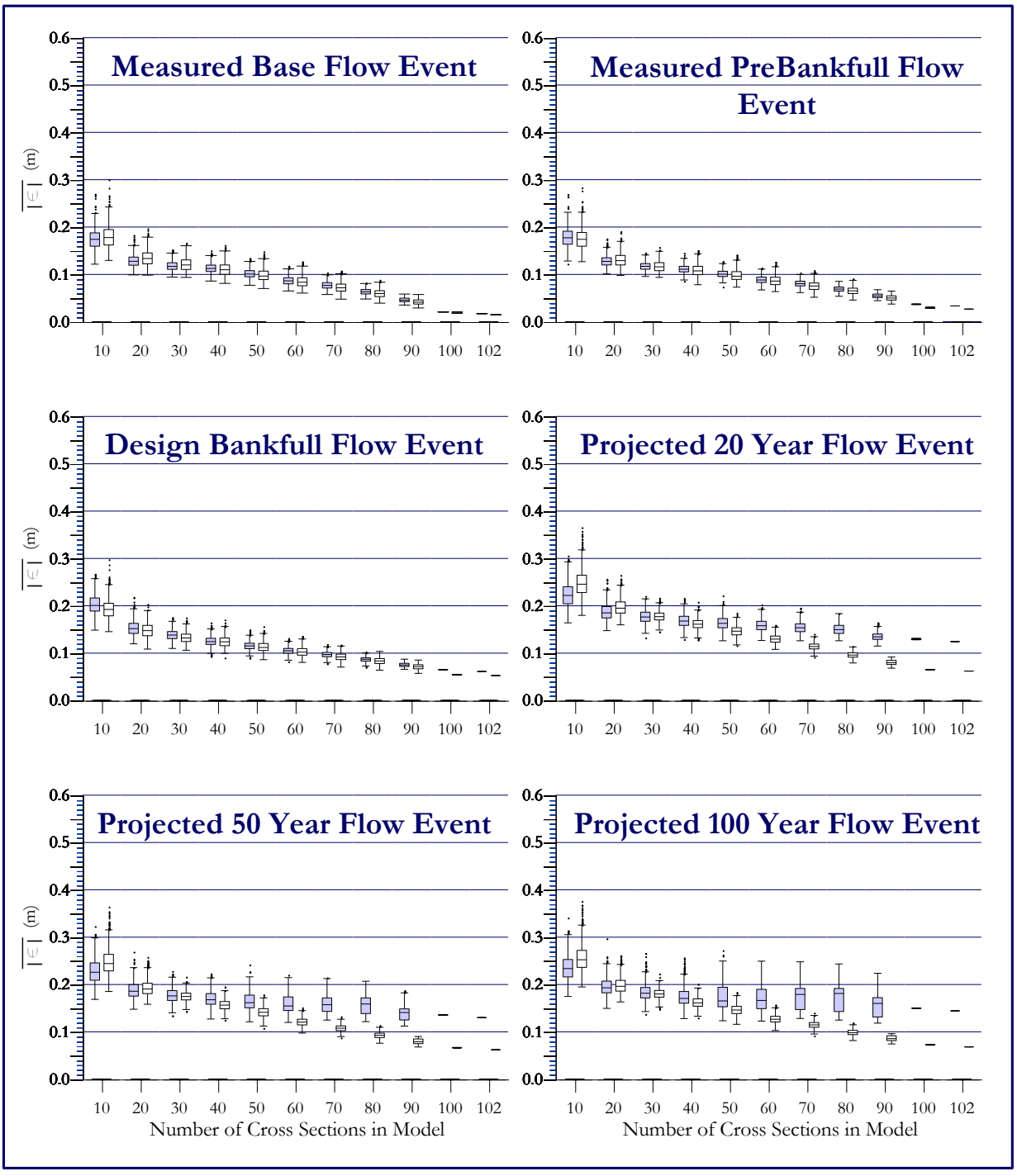

Figure 4-7. Results of Roughness Uncertainty using Low Manning's n Values in both the Main Channel and on the Overbank Areas.

absolute error observed during the projected 100-year flow event are larger than those produced using a mean Manning's n for 10 randomly added cross sections thus indicating that floodplain proper roughness estimations are very important in the resulting WSE forecasts. Contrary to the calibrated experiments, the uncalibrated results continue to decrease in absolute error for discharges greater than bankfull such that an absolute error of $\overline{|\in|} = 0.068m$ is achieved with a model employing all 102 cross sections. The WSE error for these realizations range between 0.02cm and 41cm depending on the cross section being considered and related roughness.

The separation between calibrated and uncalibrated results using low Manning's n at higher flow events is the result of using only three calibration locations and also calibrating the model for only one measured event. This difference will amplify at non-calibrating locations by recognizing that the roughness value in the denominator of Manning's equation (Equation 2.5) will increase conveyance and velocities; therefore, a smaller WSE absolute error will result if the floodplain roughness values provided in each simulation overestimate roughness as opposed to an underestimation.

A similar suite of numerical experiments were conducted for alternative cases in the over estimation of Manning's roughness for both the main channel and flood plain regions using values obtained in Section 3.1.2 and outlined in Table 4-3. The results presented in Figure 4-8 notably differ when compared to the absolute errors of low estimates of Manning's roughness coefficients across all discharges illustrated in Figure 4-7. For the cases of over estimating both main channel and flood plain roughness, the calibrated and uncalibrated results behave in a similar fashion for all discharge experiments and are consistent with the results presented in Figure 4-2. The impact of high roughness values compared to average roughness values is best portrayed in the results for the projected 100-year flow event for both calibrated and uncalibrated scenarios. For the

complete suite of 102 cross sections, the average absolute error in the water surface elevations is $\overline{|\epsilon|} = 0.107m$ and $\overline{|\epsilon|} = 0.081m$ for the calibrated and uncalibrated conditions respectively.

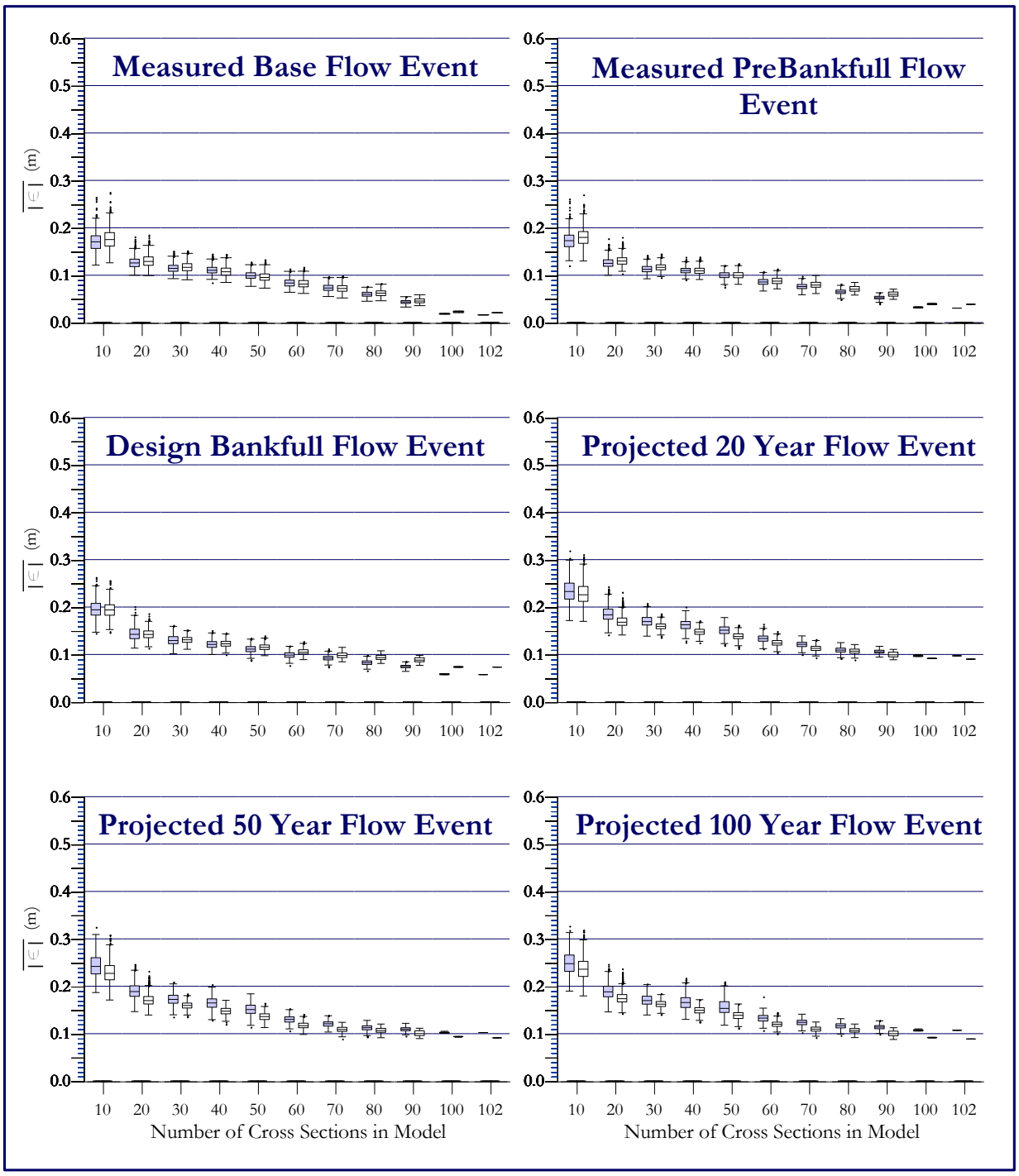

Figure 4-8. Results of Roughness Uncertainty using High Manning's n Values in both the Main Channel and Overbank Areas.

These results demonstrate that even at the largest discharge evaluated, there is no significant difference to final WSE's when over estimations of roughness coefficients occur beyond a certain level of discretization.

The final analysis carried out to examine the impact of roughness in hydraulic modelling involved using mean Manning's n values – as in the second and third axiom – in the main channel while using either a high or low Manning's n value on the overbank areas. These analyses were conducted in recognition that, although there may be some quantifiable methods of inventorying flood plain roughness (Section 2.1.3), often the practice of flood plain roughness estimation is visual, and consequently subject to considerable error. Evaluation of this scenario was carried out using the same cross section scenario analysis used in Section 4.1; however, since the effects of this analysis are only relevant when the flow surpasses bankfull discharge, only discharges exceeding bankfull discharge were evaluated. The results for this analysis are illustrated in Figure 4-9 for the projected 20, 50 and 100 year flow events.

The trends in Figure 4-9 are similar to the previous two suites of numerical experiments using exclusively either high or low roughness coefficients for both the bankfull and flood plain regions. It is noted, however, that the absolute error observed in Figure 4-9 approaches an absolute error of zero, relative to the results presented in Figure 4-7 and Figure 4-8 which is a result of the main channel roughness representing the characteristics of the second and third axioms.

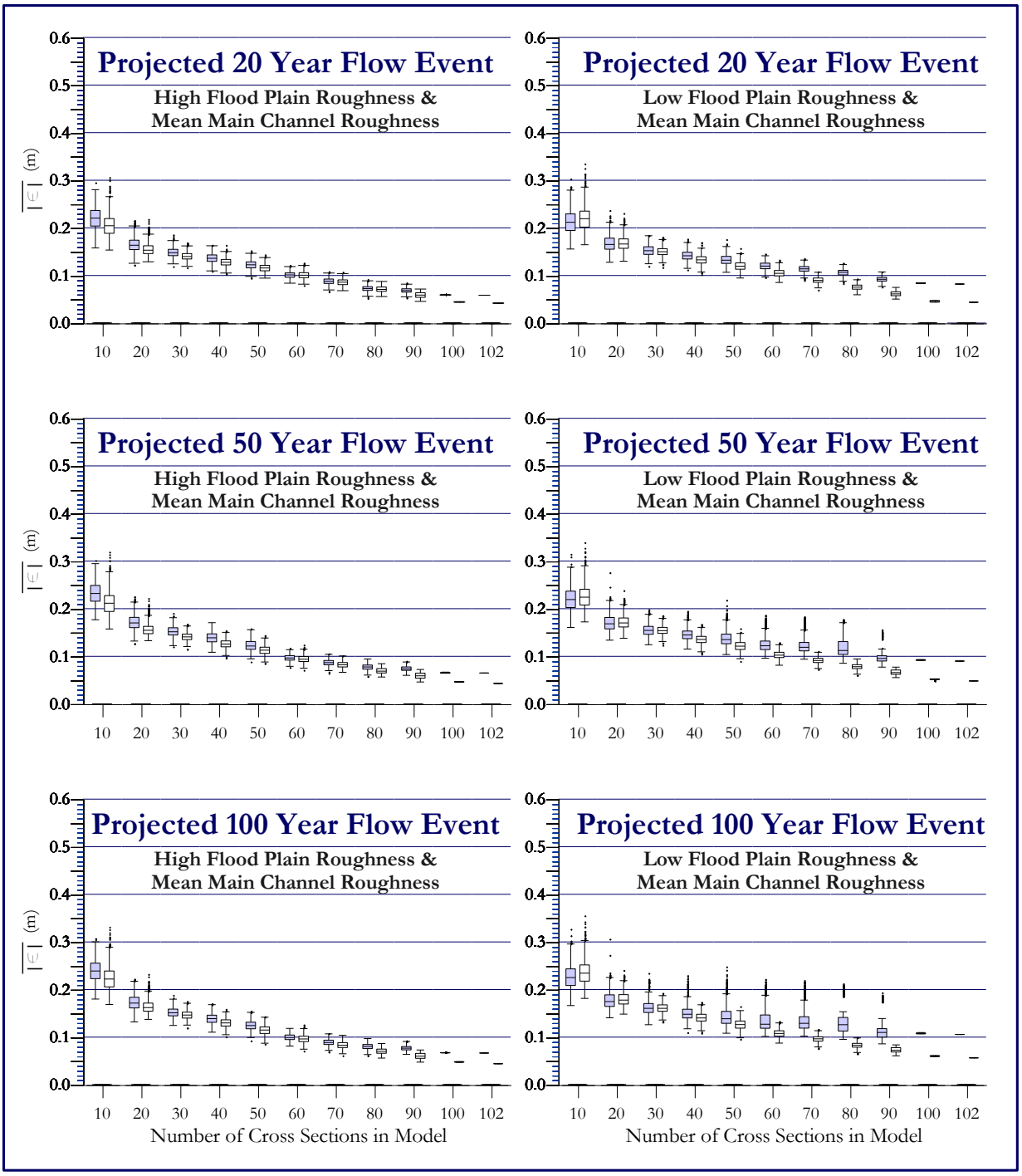

Figure 4-9. Results of Roughness Uncertainty Exclusively in Overbank Regions.

4.5 Model Error Associated with Channel Slope

The previous numerical experiments evaluated differences in WSE estimates based upon differences in discretization, cross section resolution, topographical error and roughness for the

entire reach. The previous analyses can also be stratified and re-interpreted as a function of slope class and parameter uncertainty from the other variable quantified in hydraulic modelling. For these analyses, the entire reach was stratified into three slope classes being: steep (≈ 2.11%), moderate (≈ 0.71%) and mild slope regions (≈ 0.30%).

The sampling strategy used for these numerical experiments was similar to that presented in Section 4.1 where full cross section detail was used and experiments conducted for the six discharges ranging between base flow and the projected 100-year return period. However, when random cross section sampling was employed, random sampling was limited to available cross sections within each slope class that were not required boundary or calibration sections. As previously identified, a greater number of cross sections were surveyed in the field in the steep sections relative to the lower gradient reaches, thus partially biasing the random sample frequency outcome results towards the steeper channel reaches. This is especially evident in the steep sloped zone where very little variance reduction randomization occurs once 50 cross sections are randomly added to the study reach. Regardless of potential bias, analyzing the results from a slope magnitude perspective is still of relevance to elucidate potential differences in the previous experiments when stratified by slope.

The results presented in Figures 4-10, 4-11, and 4-12 illustrate the results from the cross sectional dicretization analysis performed with mean roughness values and the highest resolution cross sectional detail for the three identified slope classes. The average absolute error ($\overline{|\in|}$) for each numerical experiment was calculated by dividing the absolute cross sectional water surface elevation error attributed exclusively in each slope zone by the number of cross section sampled within each slope zone rather than over the entire reach as undertaken in Section 4.1.

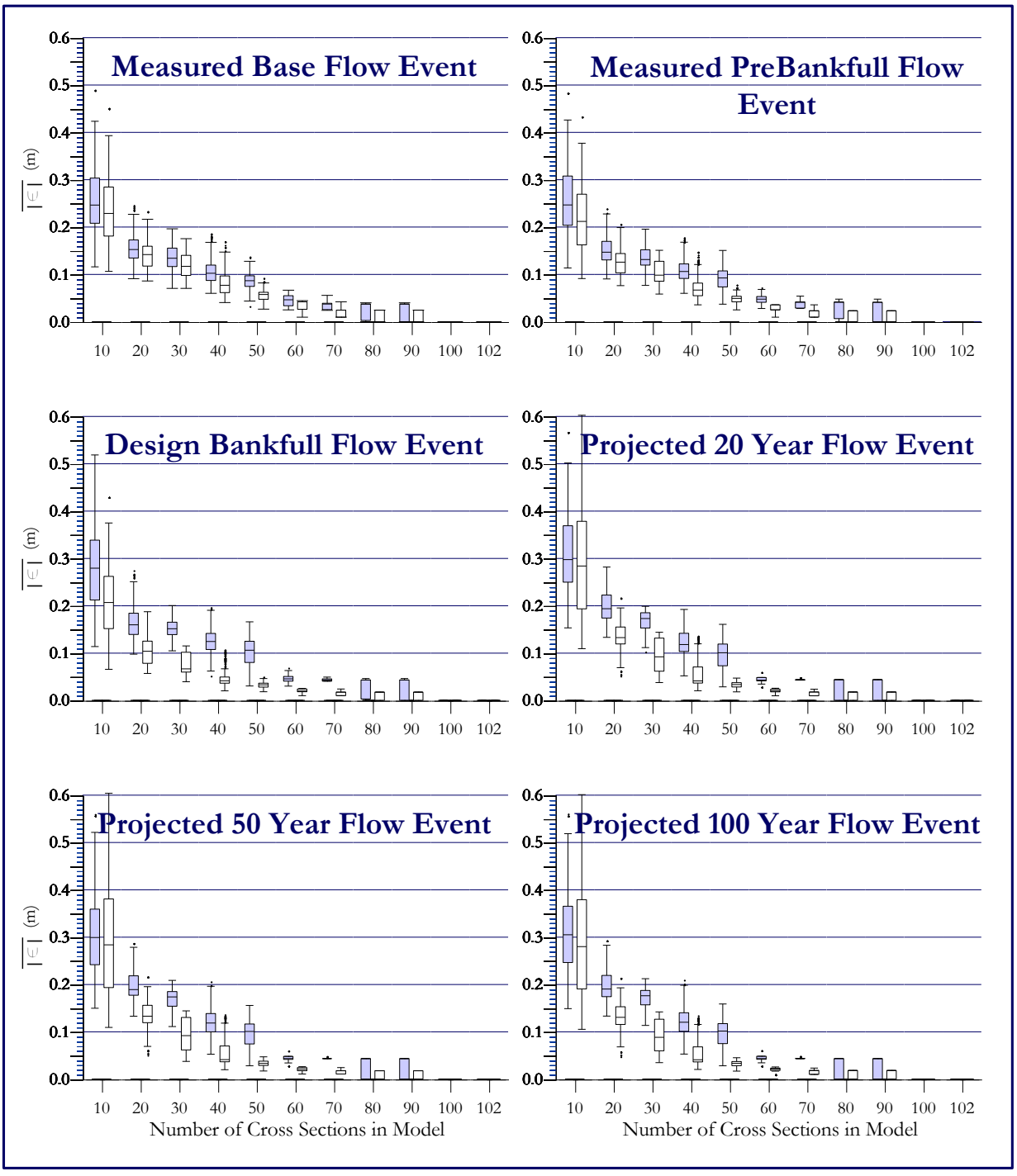

Figure 4-10. Slope Related Results for Cross Sectional Discretization using Average Roughness for the Steep Channel Slope Zone.

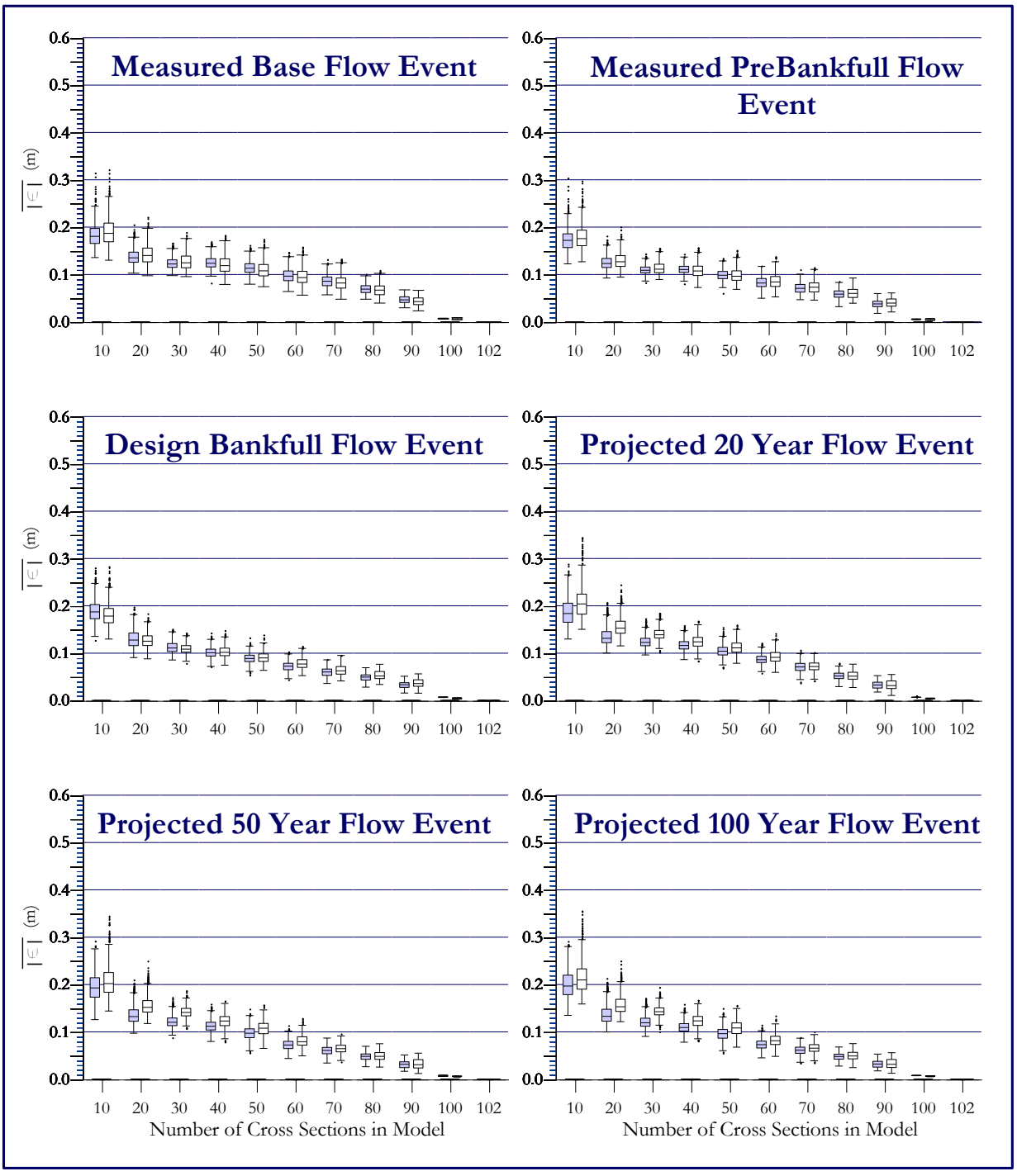

Figure 4-11. Slope Related Results for Cross Sectional Discretization using Average Roughness for the Moderate Channel Slope Zone.

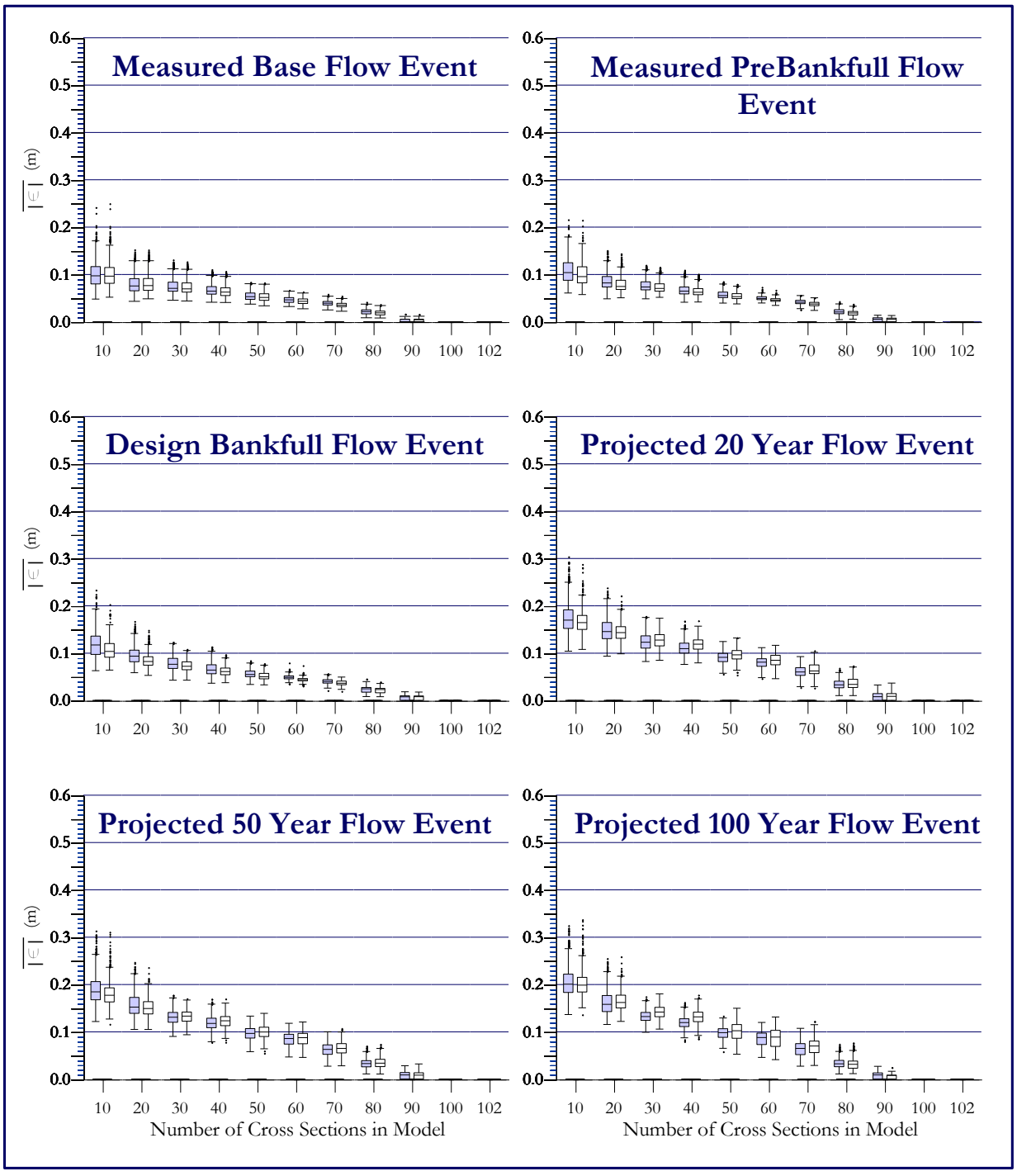

Figure 4-12. Slope Related Results for Cross Sectional Discretization using Average Roughness for the Mild Channel Slope Zone.

The most obvious notable result from these analyses is the large propagation of error which occurs in the steep sloped zone (Figure 4-10) when only 10 cross sections are randomly introduced to the entire study reach. The magnitude of this error is significantly larger than the error which occurs for the same conditions in the moderate and mild sloped zones. The result demonstrates the propagation of error with decreased cross sectional spacing is most prevalent in steep reaches compared to less lower gradient reaches. In the moderate versus mild slope regions, a similar trend is observed whereby $\overline{|\in|}$ increases with increasing slope as a function of cross section frequency. However, these results are muted relative to the steep slope condition.

Results of Figure 4-11 through Figure 4-12 generally demonstrate that as discharge increases, the differences in $\overline{|\in|}$ becomes negligible suggesting that the effects of slope do not play as a significant role in the WSE calculations, for a given cross section, relative to the flood plain roughness factors. The most notable observation of these analyses identifies that with increased channel slope, increase cross section frequency is particularly important in reducing WSE absolute error.

4.6 Relating Economics with Results

Although many of the results presented in the previous sections are obvious from an inspection of the governing equations related to one-dimensional hydraulic modelling (Equation 2-1 through Equation 2-8), the human resource investments relative to model accuracy are not always congruent with model accuracy and economics. To evaluate project economics for the suite of numerical experiments that have been considered, a number of assumptions must be made.

With respect to human resources, it is assumed that three people are needed to perform a longitudinal survey, two people to perform cross sectional profiling (i.e. leveling), two people to estimate main channel roughness, and one person to estimate overbank roughness. Based upon

time logs in conducting the field survey component of this study over a 7.6km reach for 128 cross sections where detail cross section resolution were obtained consistent with a first-order traverse survey, a task-base economic matrix was developed. It should be noted that the longitudinal traverse survey was undertaken when deciduous vegetation was dormant to minimize field time and control points. Based upon the installation of bench marks at each cross section during the traverse survey, detailed cross sectional analysis and pebble counts were conducted throughout the remainder of a summer season, where no significant decrease in the rate of data acquisition relative to vegetation density would occur. Table 4-4 outlines the human resource based effort for each of the primary tasks undertaken in the field analysis of this project.

Table 4-4. Human Resource Hours by Field Tasks.

Task	Unit of measure	Number of People	Human Resource Hours
Longitudinal Survey	**Per km**	**3**	**4.21**
Topographical Error Reduction	**Per Section**	**1**	**0.59**
Cross Section Profiling	**Per Section**	**2**	**1.86**
Main Channel Roughness Estimate	**Per Section**	**2**	**1.63**
Flood Plain Roughness Estimate	**Per Section**	**1**	**0.34**

A spectrum approach, illustrated in Figure 4-13 and Figure 4-14, provides a visual representation of the degree to which field data collection elements and sampling frequency affect model accuracy for a one-dimensional model when compared to the raw data input conditions. The spectrums presented in both figures are such that the first spectrum illustrates the weighting of error effects on a calculated WSE, the second spectrum is a weighting of recorded resource

spending from a human resource perspective, and the third spectrum is a proposed resource distribution based on the first two spectrums.

Figure 4-13 is indicative of error distribution and proposed resource distribution if flow is contained within the bankfull limits of the channel.

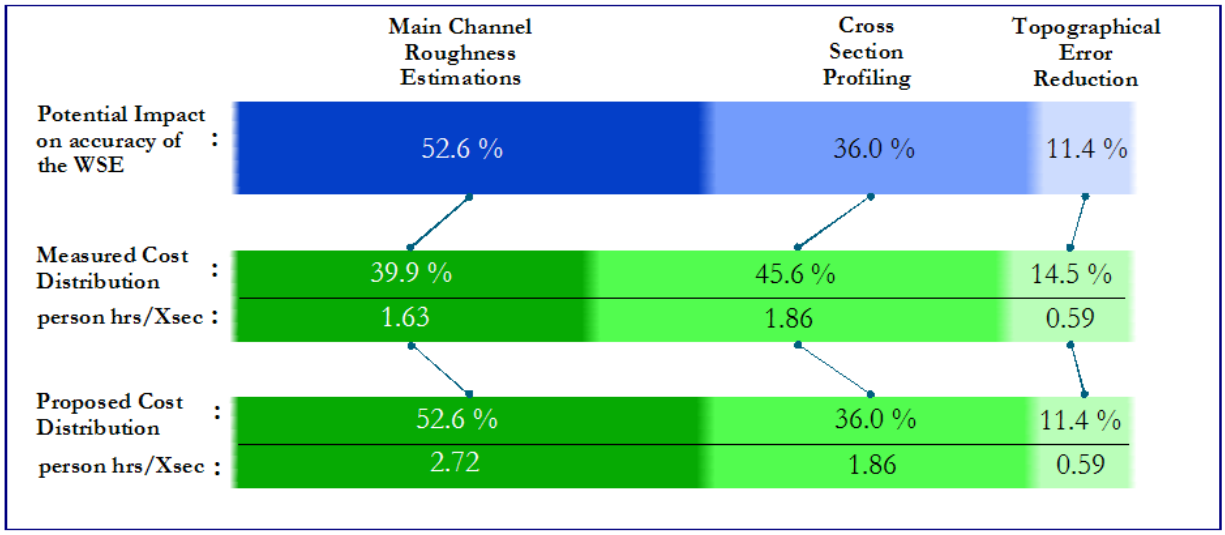

Figure 4-13. Error Effects & Proposed Data Collection Costing Spectrum For Flows Contained Within Bankfull Limits.

Results presented in Figure 4-13 were obtained through weighting of results from all of the sensitivity experiments using the three lowest flow conditions (i.e. measured base flow, measured pre-bankfull, and design bankfull). These results are indicative of the fact that most time and effort was spent on obtaining highly detailed cross section profiles at each cross section location. While the cross section profiles are important for modelling inchannel hydraulics, they do not constitute the greatest impact on the model's accuracy. Experimental results indicate that accurate roughness estimation will increase the accuracy of the computed WSE more so than the other input variables; therefore, it is proposed that the resource distribution and time required to estimate this roughness be increased to coincide with the quantitative error weighting results.

When flows greater than bankfull are considered, the overbank roughness estimation plays a significant role in the accuracy of the computed WSE. Figure 4-14 reflects the error distribution and proposed resource distribution for the case when flows are great enough to spill over the main channel and spread out into the flood plain.

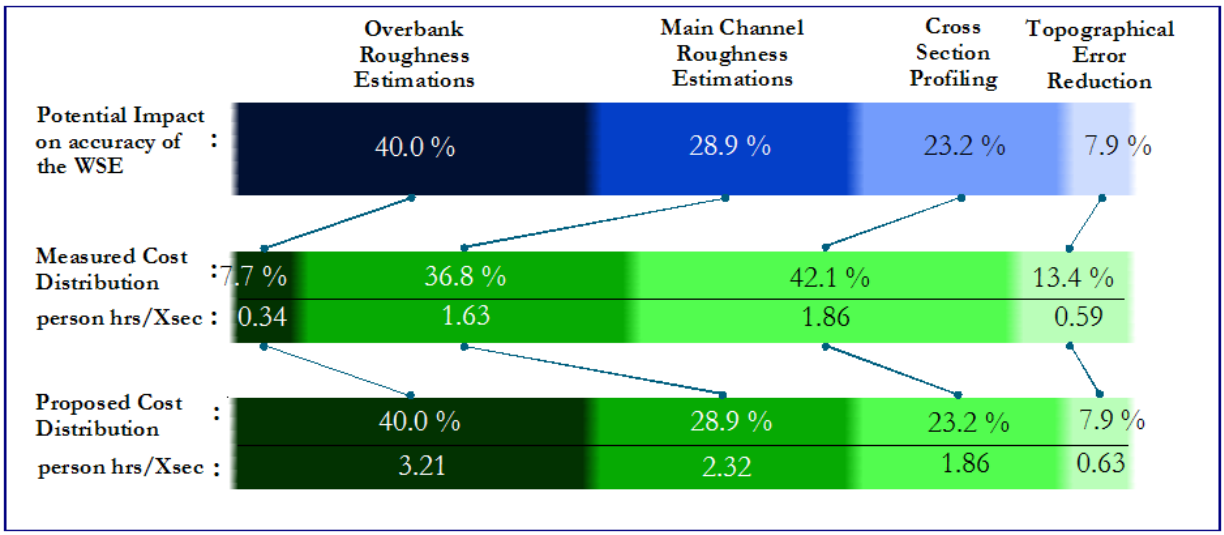

Figure 4-14. Error Effects & Proposed Data Collection Costing Spectrum For Flood Flow Conditions.

The spectrum presented in Figure 4-14 illustrates the importance of overbank roughness estimates when flows exceed the bankfull level. This spectrum also shows the minor resource investment that goes into aquiring these estimates when compared to the hydraulic modelling project's resource distribution as a whole. To increase the potential for greater WSE accuracy, it is proposed that resource investment be increased for overbank roughness estimates such that the proposed cost distribution is in line with the error impact wieghting.

It is worth noting that the results presented in Figure 4-13 and Figure 4-14 are based on weighting of median values from results presented throughout this chapter. The resource distributions in

both figures are based on two field seasons where practices were repeated so that an average resource expenditure could be calculated and used to quantifiably weight the results.

CHAPTER 5. CONCLUSION

The results presented throughout this report are founded on close to one million hydraulic simulations of the study reach. This extensive analysis provides a quantitative understanding of the sensitivity of hydraulic modelling input variable (i.e. topographic, roughness, and flow) relative to the location that was investigated. The location used for this study provided a diverse set of input data; and although all results are case study specific, the results can – with an understanding of their origin – go beyond the study location and be used to better manage other hydraulic modelling projects.

The vast majority of results are integrated over 1000 sets of randomly sampled cross section locations along a river reach and each of these random sets roughly represents the sample locations that might be selected by a different hydraulic engineer. Results demonstrate that as cross sectional frequency along the reach increases, the model error decreases. A decrease in model accuracy of 0-5 mm was observed per meter of spacing between cross sections. The model accuracy of bankfull flows and below is somewhat less sensitive to changes in cross sectional frequency than the accuracy of overbank flow events, which was shown to be controlled by the representative overbank roughness inputs. The modelling error caused by scarcely surveyed cross sections predominates the error caused by minimal cross section detailing that can miss irregularities in the cross section. Therefore, results show that when project resources dictate a limited survey effort, modelling accuracy is higher when the survey is focused on maximizing the number of cross sections with minimal detail as opposed to precisely characterizing a smaller number of cross sections. Also, the practice of high order surveying (i.e. 1st Order) was not justified from the results of this study due to its minimal improvement in topographical accuracy when compared to the model's topographical definition as a whole. When results are disaggregated into steep, moderate and mild slope classes, they show that with increasing channel

slope, an increase cross section frequency is particularly important in reducing WSE absolute error. For example, very few cross sections in steep reaches lead to WSE absolute errors that are 2-3 times higher than the errors in moderate to mild slope classes for a comparable number of modelled cross sections. Lastly, the results do not change substantially between the calibrated and uncalibrated model axioms. This indicates that the results are similar in our case study regardless of whether the model was calibrated or just applied under initial roughness estimates. However, it should be emphasized that calibrated results were for discharges significantly less than bankfull: hence the significance of model calibration at regulatory levels (i.e. 100-year return period) can not be quantified at this stage of the research.

When the results are contrasted with resource requirements for two consecutive field seasons, the study indicates that additional emphasis needs to be placed on accurately representing the overbank roughness if greater accuracy in flood stage is of particular interest. Further, the time and effort allocated to high order survey protocols pales in comparison to improved estimates of floodplain roughness estimates when accuracy in flood stage water surface elevations are of primary interest.

DIGITAL APPENDIX A

Contents for this appendix are provided in digital format in the media pocket at the back of the report. All appendices are only available in hard copy format.

BIBLIOGRAPHY

Ackers, P., White, W.R., Perkins, J.A., Harrison, A.J., (1978). *Weirs And Flumes For Flow Measurement*. John Wiley & Sons Ltd., New York, NY, 34-42.

Anderson, A.G., (1970). "Tentative Design Procedure For Riprap-Lined Channels." National Coopertive Highway Research Program Report, 108, pp. 17-40.

Balena, F., (2006). *Programming Microsoft® - Visual Basic 2005: The Language*, 2005 Edition. Microsoft Press, Redmond, Washington, 439-671.

Bradley, J., Peterka, A.J., (1957). "The Hydraulic Design of Stilling Basin: Hydraulic Jumps on a Horizontal Apron." JHYD, ASCE, Vol. 83, No. 5, pp. 1-24.

Brogly, P.J., Martini, I.P., Middleton, G.V., (1998). "The Queenston Formation: shale-dominated, mixed terrigenous-carbonate deposits of Upper Ordovician, semiarid, muddy shores in Ontario, Canada." Canadian Journal of Earth Science, Vol. 35, pp. 702-719.

Brovelli, M.A., Crespi, M., Fratarcangeli, F., Giannone, F., Realini, E., (2008). "Accuracy assessment of high resolution satellite imagery orientation by leave-one-out method." ISPRS Journal of Photogammetry & Remote Sensing 63, pp. 427-440.

Buchanan, T.J., Somers, W.P., (1969). *Techniques of water-resources investigations of the United States Geological Survey – Chapter A8 Discharge measurements at gaging stations*, United States Department of the Interior, Washington D.C.

Burke. R., (2003). *Getting To Know ArcObjects™ - Programming ArcGIS® with VBA*. ESRI Press, Redlands, California, 227-357.

Chagas, P., Souza, R., (2005). "Solution of Saint Venant's Equation to Study Flood in Rivers, through Numerical Methods." Hydrology Days, pp. 205-210.

Chapman, L.J., Putnam, D.F., (1984). *The Physiography of Southern Ontario*, Third Edition. Government of Ontario, Toronto, Ontario, 101, 114-122, 190.

Chaudhry, M.H., (2008). *Open-Channel Flow*, Second Edition. Springer Science+Business Media, New York, NY, 55-318.

Chow, V.T., (1959). *Open Channel Hydraulics*. McGraw-Hill Book Company, Inc., New York, NY, 109-123.

Corani, G., Guariso, G., (2005) "Coupling fuzzy modelling and neural networks for river flood prediction." IEEE Transactions on Men, Systems and Cybernetics part C, 35(3), pp. 382-391.

Dalrymple, T., Benson, M. A., (1967). Measurement of peak discharge by slope- area method. *: U.S. Geological Survey Techniques of Water-Resources Investigations*. United States Department of the Interior, Washington D.C., Book 3, chap. A2, 12.

Dodge, D.P., Mellquist, P., Edwards, A., (1994). *The Rivers Handbook – Hydrological and Ecological Principles*. Blackwell Science Ltd., Osney Mead, Oxford, 187-196.

Dooge, J.C., (2007). "The occurrence and movement of water." Acta Geophysica, vol. 55, no. 3, pp. 344-358.

Ghani, A.B., Azazizakaria, N., Kiat, C.C., Ariffin, J., Hasan, Z.A., Ghaffar, A.B.A., (2007). "Revised equations for Manning's coefficient for sand-bed rivers." International Journal of River Basin Management, Vol. 5, No. 4, pp. 329-346.

Haestad, Dyhouse, G., Hatchett, J., Benn, J., (2003). *Floodplain Modeling Using HEC-RAS*, First Edition. Haestad Methods, Inc., Waterbury, CT, 13-312.

Henderson, F.M., (1966). *Open Channel Flow*. Macmillan Publishing Co., Inc., New York, NY, 174-227, 285-346.

Holzner, S., (2006). *Visual Basic 2005 – Black Book*. Dreamtech Press, New Delhi, 83-114, 433-544.

Julien, P.Y., (2002). *River Mechanics*. Cambridge University Press, Cambridge, NY, 88-152.

Kavanagh, B.F., Glen Bird, S.J., (1989). *Surveying – Principles and Applications*, Second Edition. Prentice-Hall, Inc., Englewood Cliffs, New Jersey, 1-243.

Maidment, D.R., (1993). *Handbook of Hydrology*. McGraw-Hill, Inc., New York, NY, 19.1-19.26.

Montgomery, D.R., Panfil, M.S., Hayes, S.K., (1999). "Channel-bed mobility response to extreme sediment loading at Mount Pinatubo." Geology, Vol. 27, No. 3, pp. 271-274.

Mooney, D.M., Holmquist-Johnson, C.L., Broderick, S., (2007). *Rock Ramp Design Guidelines*. U.S. Department of the Interior – Bureau of Reclamation, Denver, Colorodo, 11-15.

Natural Resources Canada, (1978). *Specifications and Recommendations for Control Surveys and Survey Markers*. Canada Centre for Remote Sensing – Geodetic Survey Division, Ottawa, Ontario, 6-13.

Ormsby, T., Napoleon, E., Burke, R., Groessl, C., Feaster, L., (2001). *Getting To Know ArcGIS® desktop*, Second Edition Updated for ArcGIS 9. ESRI Press, Redlands, California, 357-460.

Press, W.H., Flannery, B.P., Teukolsky, S.A., Vetterling, W.T., (1986). *Numerical Recipies – The Art of Scientific Computing*. Cambridge University Press, New York, NY, 191-225.

Reich, Y., Paz, A., (2008). "Managing product quality, risk, and resources through resource quality function deployment." Journal of Engineering Design, Vol. 19, No. 3, pp. 249-267.

Reinfelds, I., (1997). "Reconstruction of changes in bankfull width." Applied Geography, Vol. 17, No. 3, pp. 203-213.

Rice, S., Church, M., (1996). "Sampling Surficial Fluvial Gravels: The Precision of Size Distribution Percentile Estimates." Journal of Sedimentary Research, Vol. 66, No. 3, pp. 654-665.

Strum, T.W., (2001). *Open Channel Hydraulics*. McGraw-Hill Companies, Inc., New York, NY, 98-305.

Tung, Y.K., Yen, B.C., Melching, C.S., (2006). *Hydrosystems Engineering Reliability and Risk Analysis*. McGraw-Hill Companies, Inc., New York, NY, 289-335.